STABLE REFERENCE TRAJECTORY MODIFICATION FOR HANDLING ACTUATOR FAILURE IN CONTROL SYSTEMS

by

IFEOLU OLALEKAN OGUNLEYE

Presented to the Faculty of the Graduate School of
The University of Texas at Arlington in Partial Fulfillment
of the Requirements
for the Degree of

MASTERS OF SCIENCE IN AEROSPACE ENGINEERING

THE UNIVERSITY OF TEXAS AT ARLINGTON

December 2011

To my mother and father Bode and Funmi Ogunleye

who set the example and sacrificed much on my behalf.

ACKNOWLEDGEMENTS

First, I would like to thank my supervising professor Dr. Kamesh Subbarao for constantly inspiring and guiding me, and also for his invaluable advice during the course of my master studies. His passion and zeal for research served as a stimulus during the many years of the masters research. I wish to thank committee members Dr. Panayiotis Shiakolas, and Dr. Don Wilson both of which have been highly influential my entire time at the University of Texas Arlington.

I would also like to extend my appreciation to the Department of Defense for providing financial support for my masters studies. I wish to thank Colonel Denis Hunt and Colonel James Feck for providing funding while I was employed with the Defense Contract Management Agency.

Finally, I would like to thank my family, for all the support they provided over the last several years. I am extremely grateful to my mom, dad, brother and sister for their prayers and guidance in my life. I would like to express my deepest love and gratitude to my wife who has stood by my side over the final stages of my masters. Her steadfast love and patience in all my pursuits have been greatly cherished.

Novermber 18, 2011

ABSTRACT

STABLE REFERENCE TRAJECTORY MODIFICATION FOR HANDLING ACTUATOR FAILURE IN CONTROL SYSTEMS

IFEOLU OLALEKAN OGUNLEYE, MS

The University of Texas at Arlington, 2011

Supervising Professor: Kamesh Subbarao

The issue of rapidly reconfiguring the reference trajectory under unanticipated actuator failures in order to regain lost performance or aircraft handling qualities is explored. The failures detected in real-time are compensated for by ensuring the input to the system reflects current system conditions. This thesis will also show that only the general structure of the failed system component is needed to achieve successful failure detection and reference trajectory reconfiguration. This approach allows the nominal control structure to remain unchanged in the presence of changing flight and system conditions. Acceptable system performance is recovered by detecting the actuator failures in real-time. The benefit of this approach is that the modification does not alter the control gains of the closed loop system which eliminates the apprehensions associated with most adaptive control techniques. The implementation of this technique will be done on a linear longitudinal model of an F-16 like aircraft and the efficacy of the basic approach will be shown through computer simulations.

TABLE OF CONTENTS

LIST OF ILLUSTRATIONS

CHAPTER 1

INTRODUCTION

1.1 Introduction and Motivation

Accommodating real time failures in flight control systems (FCS) has been an active area of research for quite some time. As the complexity of FCS' increase, the need to design a fault tolerant system increases accordingly. A fault tolerant system is a system that is able to continue operation, possibly at a reduced level, rather than failing completely when different components within the standard flight control system fails.

In the past several years there has been extensive research and breakthroughs in the design and implementation of reconfigurable control systems. Reconfigurable control systems are a means of producing a fault tolerant system. There are other means of achieving a fault tolerant system such as robust control [1]. The different between robust control and reconfigurable control is this: a robust controller is a fixed control system designed to accommodate variations within a system or its operating environments, while reconfigurable control is designed to change or adapt based on variations within a system or its operating environments. The goal of a reconfigurable control system is to achieve an automated, quick system reconfiguration as a response to sudden unexpected variations or changes within the system itself or its operating environment [2–4]. The ultimate aim of the system reconfiguration is to reclaim as much of the control performance as possible after a fault has occurred in the controlled system.

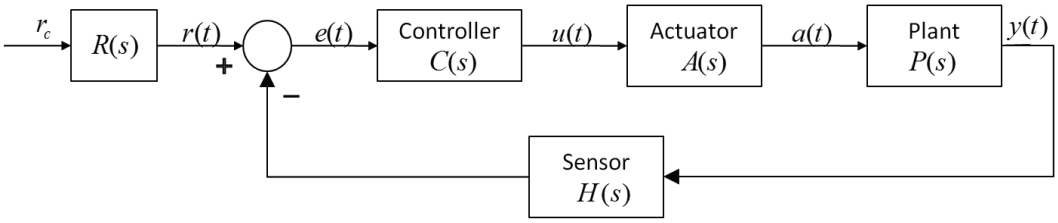

Figure 1.1. Generic closed loop system.

At present, there are several approaches in reconfigurable flight control systems being researched, many of which have an ability to maintain aircraft performance or stability in the presence of different forms of system failures [1, 4–9]. These approaches are categorized by the components being reconfigured: those within the closed loop system [1, 6, 10, 11] and those outside of the closed loop [4, 9, 12]. This is an important distinction to make when considering fault tolerant designs by means of system reconfiguration. One common approach utilizes the effectiveness of adaptive controllers [6, 8, 13], a special type of nonlinear control system which can alter its parameters to adapt to a changing environment, such as variations in process dynamics, failures introduced to the system, or other general disturbances. The mechanisms for adjusting these parameters online are based on signals within the system.

1.1.1 Controller Reconfiguration Methods

Figure 1.1 shows the structure of a generic closed loop system with $C(s)$, $A(s)$, $P(s)$, and $H(s)$ representing the controller, actuator, plant, and sensor respectively which are all the components that make up the closed loop. While, $r_c(t)$ is the commanded input to the system; $R(s)$ is the input transfer function that generates $r(t)$, the reference trajectory. The first and most common type of reconfiguration is one

which restructures, or reparameterizes, the controller or other components within the closed loop system. This generally means altering the controller or sensor block in Figure 1.1. These types of reconfiguring interventions include control algorithms, sensory data processing algorithms and actuator control allocation algorithms. It very common for a fault tolerant system to include a Fault Detection Isolation Recovery (FDIR) system and a Health Monitoring System (HMS) to aid in the task of reconfiguration, while the actual reconfiguration is carried out by an adaptive controller. A FDIR system is a combination of fault detection, fault isolation, and fault recovery [1]. Fault detection monitors the controlled system and detects if there is any failure. Fault isolation finds the location of the failure or determines which component within a system has failed and, depending on the complexity, supplies quantitative parameters of the failure. Fault recovery provides control system adaptation to the failure. While an HMS monitors a large number of both critical and non-critical components, its goal is to monitor the overall progress of the controlled system and to make further tasking decisions in accordance with current system conditions and the overall system and control objective.

A fault tolerant system which utilizes both a HMS and a FDIR is shown in [1]. Here, a robust integrated fault-tolerant flight control system is shown to accommodate different types of actuator failures and control effectors' damage while rejecting disturbances. This is done by first using a decentralized FDIR system. In addition, a HMS integrated with an adaptive reconfigurable controller is used to accommodate a large class of failures. The use of the adaptive reconfigurable controller is to effectively compensate for the effect of a class of possible failures detected by the FDIR and HMS. In [1] it is shown the system achieves acceptable performance in the presence of two locked actuators, two damaged control effectors, and a large disturbance affecting all three angular rates.

A similar method that also uses an adaptation based reconfiguration is shown in [10]. In their work, Hess and Siwakosit develops a method for accommodating a set of actuator failures that change the parametric model of the actuator which causes deterioration in actuator performance. An adaptation logic is designed by an identification technique which considers post failure system responses to a test square-wave input. The static gain term varies until the response meets a certain overshoot criterion. This work is extended to Multi-Input Multi Output (MIMO) systems in [14]. This is made possible by utilizing a robust controller and an adaptive filter. The adaptive filter is placed in series with a Quantitative Feedback Theory compensator which employs the inherent robustness of the nominal flight control system in the presence of plant uncertainties. Their work showed significant improvement in tracking performance in the presence of actuator failure.

A similar improvement in tracking performance was shown in [6]. The method in [6] uses an adaptive controller design method based on neural networks to compensate for control effectiveness. A general structure for a neural-network-based adaptive control law was shown under the assumption that the dynamics in the system are not precisely known. The control scheme shown in [6] combines a conventional backstepping controller with neural network to guarantee the stability and robustness of closed-loop system under the condition of control surface damage.

1.1.2 Reference and Controller Reconfiguration Methods

It is possible to design a fault tolerant system not only by restructuring the controller, $C(s)$ in Figure1.1, but also reshaping the reference trajectory $r(t)$, or the input that is seen by the system. With the increasing popularity of adaptive controllers being implemented for the use of fault tolerance, special care is needed to ensure continuous adaptation and accurate convergence of the adapting parameters.

Under the effects of saturation, adaptive controllers will likely produce unfavorable results. Adaptive control usually assumes full authority control(no saturation), and generally lacks an adequate theoretical treatment for control in the presence of actuator saturation limits [11]. In most adaptive control formulations the adaptation rate is reduced or the adaptation is completed stopped to accommodate for the saturation. In [11] a methodology for adaptive control that prevents the adaptation gains from drifting due to control saturation is addressed. The reference trajectory is modified upon saturation of the actuator. The modified trajectory closely approximates the original trajectory without saturating the actuator. In [2], Jung examines the effectiveness of an Artificial Neural Network (ANN) as a compensator for the difficult problem of Cartesian space control. In [2], a rotary robot manipulator was subject to various model uncertainties which ordinarily resulted in poor tracking performance. Three possible locations at which the ANN compensation signals can be placed in the robot controller was explored. The three locations were at the actuator, at the control output, and at the input trajectory. It was found that using ANN to modify the reference trajectory to compensate for model uncertainties was the most effective. The trajectory modification scheme is also shown to be far less complicated to implement.

In [13], a method is presented that allows for simultaneous parameter estimation, real time trajectory determination, and adaptive closed loop control. Adaptive reshaping of the trajectory is accomplished in the presence of altered dynamic characteristics due to unexpected damage to the system. This is done by using an inverse dynamics method that uses pseudo forces to facilitate dynamic inversion. This approach was able to generate new feasible trajectories to be tracked while avoiding actuator saturation.

1.1.3 Reference Only Modification Methods

A fault tolerant design can be achieved without a reconfiguration or adaptation taking place within the closed loop of the system. This approach strictly focuses on gaining performance by modifying components of the system outside of the closed loop, which are $R(s)$ and $r(t)$ in Figure 1.1. Glattfelder el al. in [4] discuss reference conditioning. Here the basic idea is to modify the input to a PI controller, such that the conditioned input does not saturate the actuator. This is called the "realizable reference". The closed loop stability is determined by examining the characteristic equation from the anti-windup feedback loop [4]. The results of this study show that actuator windup is prevented; however, there are large overshoots in plant response. The overshoot depends on conditions at the time of saturation and on the eigenvalues of the linear closed loop system.

A method presented by Singla et al. in [9] shows it is possible to improve tracking performance by modifying the reference model in a model reference adaptive control law. The adaptation of the controller gains, in the presence of actuator saturation constraints; result in a modified reference trajectory and not an adaptation of controller gains. The adaptation algorithm is developed by seeking to minimize the difference between the nominal and the saturated response. And finally, in [15] an approach is implemented in which the optimal feasible reference trajectory is determined in real-time for executing a specified maneuver by an Uninhabited Aerial Vehicle. Though fault tolerance is not directly addressed the trajectory is developed while considering flight condition constraints and saturations limits.

1.1.4 Verification and Validation (Reference only Modification vs Other Methods)

In most reconfigurable flight control schemes the emphasis is placed on the re-calculation of controller gains in the presence of actuator saturations or some sort

of component or system failure. Due to the nonlinear and dynamic nature of an adaptive control system, traditional Verification and Validation (V&V) and certification techniques are not sufficient for adaptive controllers, which is a big barrier in their deployment in the safety-critical applications. V&V is a process to ensure the flight control software is safe and reliable. The actual use of adaptive controllers or neural networks in safety critical areas is still severely limited. A major reason for that is that each piece of software in a safety critical application needs to undergo a software development process which requires extensive and rigorous V&V of the software. Usually, a specific software certification procedure has to ensure that under all circumstances, the system works reliably and without failures. For example, all safety critical software for U.S. commercial avionics has to be certified by the FAA, in accordance with the RTCA DO-178B standard. The issue with adaptive reconfigurable controllers is that you are changing in real-time the closed loop structure or parameters of the system, which greatly intensifies the level of design effort and the developmental cost due to the necessary software V&V that will be required to certify the system. The standard adaptive reconfigurable control comes with its wide range of concerns, most of which deal with guaranteed performance and/or stability during reconfiguration of the control law which hinders the verification and validation of most reconfigurable control procedures.

1.2 Summary of Contributions

In this thesis the hindrances which have been coupled to reconfigurable flight control systems will be circumvented. This thesis addresses the issue of rapidly developing reference trajectories for systems with unknown actuator parameters or unanticipated actuator saturation. By reconfiguring the input to the control system ($r(t)$ in Figure 1.1), it is shown it is possible to delay or avoid divergence of the system

while maintaining the nominal control structure and gains intact. The reshaping of the reference trajectory is based on the changes/failures occurring in real-time. This is accomplished by three different approaches which use combinations of model inversion and an Extended Kalman Filter (EKF). Some preliminary results have been shown in the publication below.

I. Ogunleye and K. Subbarao,"Stable Reference Trajectory Modification for Handling Actuator Saturation in Control Systems," in *Proc. Info Tech*, AIAA 2005-6436, St. Louis, Missouri,Mar 15-18, 2011

CHAPTER 2

NOMINAL SYSTEM SPECIFICATION

In order to begin the discussion on reference trajectory modification (RTM) the nominal system must be defined. An important feature of this approach is that it is designed to work with a large class of existing systems. In this thesis the simulations are shown for a Single-Input Single-Output system (SISO) with a linear F-16 longitudinal model. This approach requires the general structure and the order of the system components to be known. It also necessitates the availability of system variables for parameter identification. With these conditions satisfied any arbitrary stable closed loop system can have this architecture applied without any alteration to the original system.

The block diagram in Figure 2.1 describes the system while operating under nominal conditions, where $C(s)$, $A(s)$, and $P(s)$ represent transfer functions modeling the controller, actuator, and the plant respectively and $e(s)$, $u(s)$, $a(s)$, and $y(s)$ are all single valued functions. The controller, actuator and plant are described by the following transfer functions;

$$C(s) = \frac{n_C(s)}{d_C(s)} \tag{2.1}$$

$$A(s) = \frac{n_A(s)}{d_A(s)} \tag{2.2}$$

$$P(s) = \frac{n_P(s)}{d_P(s)} \tag{2.3}$$

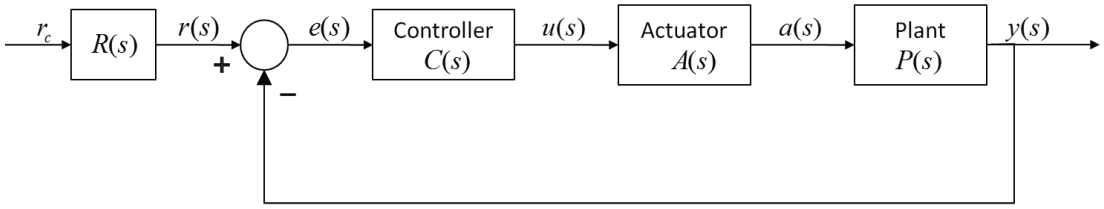

Figure 2.1. Generic closed loop system.

The closed loop system showing the input output relationship is shown in Equation 2.4.

$$\frac{y(s)}{r(s)} = \frac{P(s)A(s)C(s)}{1 + P(s)A(s)C(s)} \tag{2.4}$$

The basic closed loop structure shown in Figure 2.1 will be used to demonstrate the reference modification scheme. It is a requirement that closed loop stability is achieved under nominal conditions. It is assumed that the needed controller for precision tracking has been designed for nominal conditions. For this thesis a Proportional-Integral-Derivative (PID) controller was selected in order to address a wide range of linear controllers that are commonly encountered. A second order actuator is used to provide inputs to the plant. For the plant, a second order linear F-16 longitudinal model obtained from [16] is used to demonstrate the modification. Under nominal conditions this actuator is determined to provide adequate control action and bandwidth to achieve the commanded pitch rate trajectory. The control gains used for the controller are determined based on nominal system conditions. The plant, actuator and controller are used to form a pitch rate Command Augmented System (CAS). This system is pitch rate controller is shown in Figure 2.1. The results from this system operating under nominal conditions are shown in Figures 2.3 and 2.4.

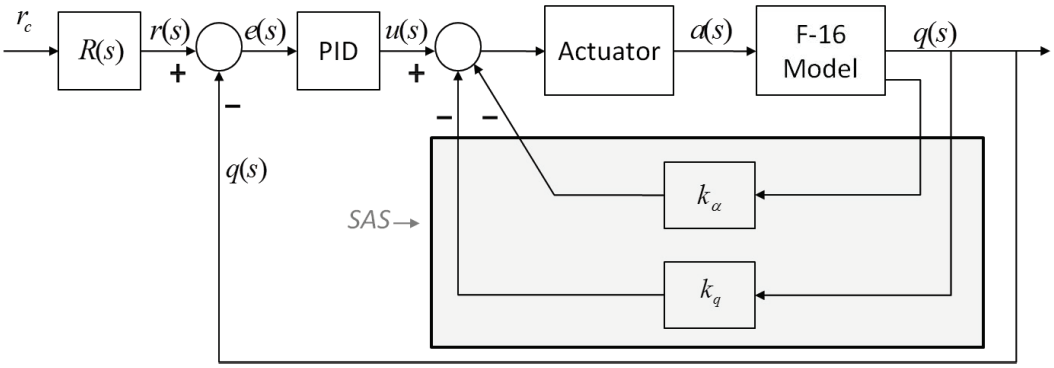

Figure 2.2. Pitch rate controller.

Figure 2.3 shows how the pitch rate CAS responds to a step input. The commanded step input of 5 deg/sec is tracked accurately. The plot in Figure 2.4 shows how the actuator position responds to the demand requested for by the controller. The plot shows that the actuator position $a(t)$ is able to track the output from the PID controller at all times.

Similar results can be seen in Figures 2.5 and 2.6. In these figures, the input to the CAS is a sinusoidal function with an amplitude of 5 deg/sec. Again the response of the F-16 linear model shows a pitch rate that tracks the reference input. Figure 2.6 shows that the second order actuator is able to match the control demand necessary for precision tracking.

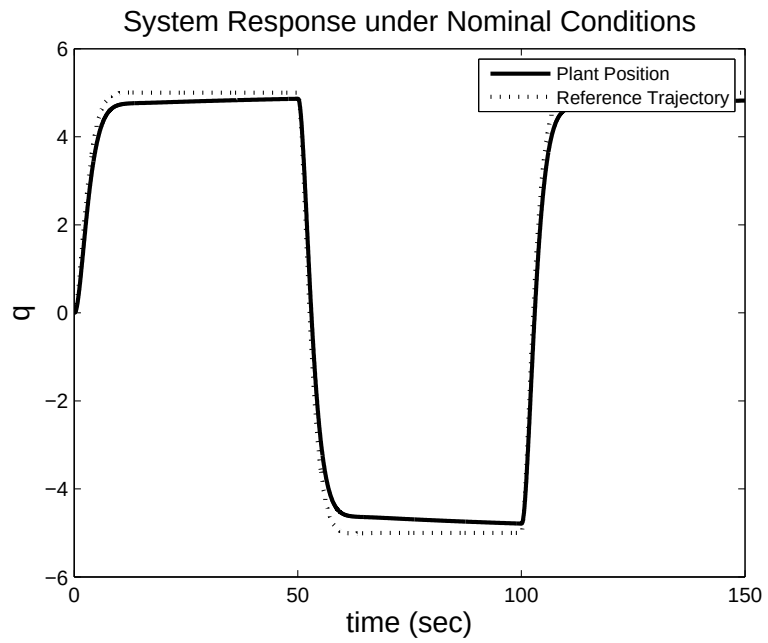

Figure 2.3. Pitch rate response with no failure (step input).

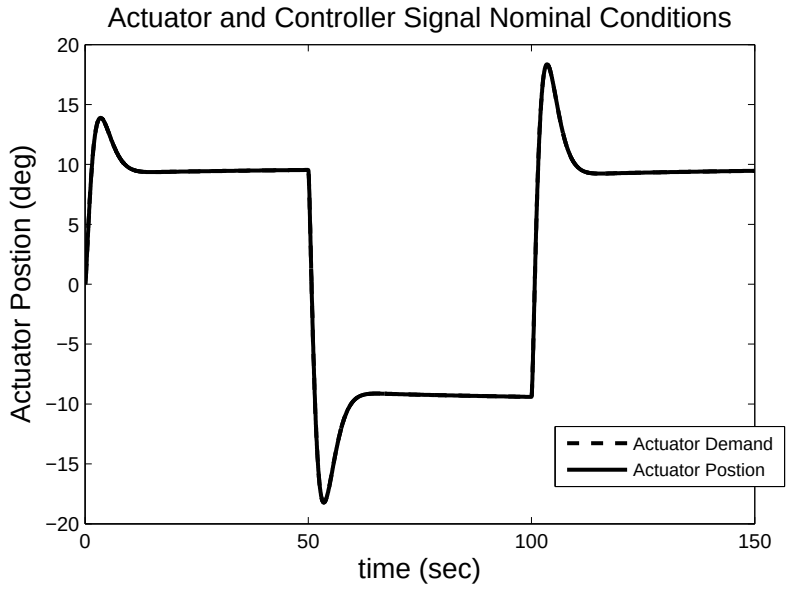

Figure 2.4. Actuator and controller output with no failure (step input).

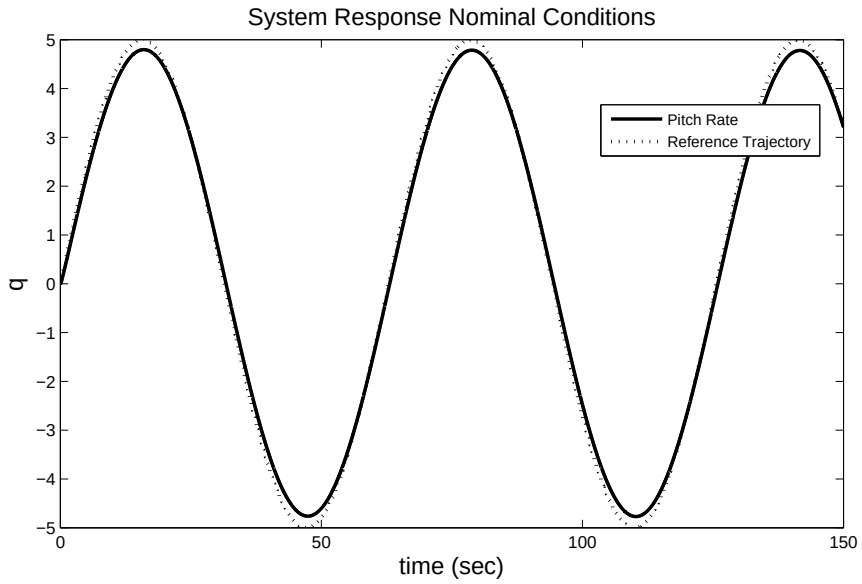

Figure 2.5. Pitch rate response with no failure (sine input).

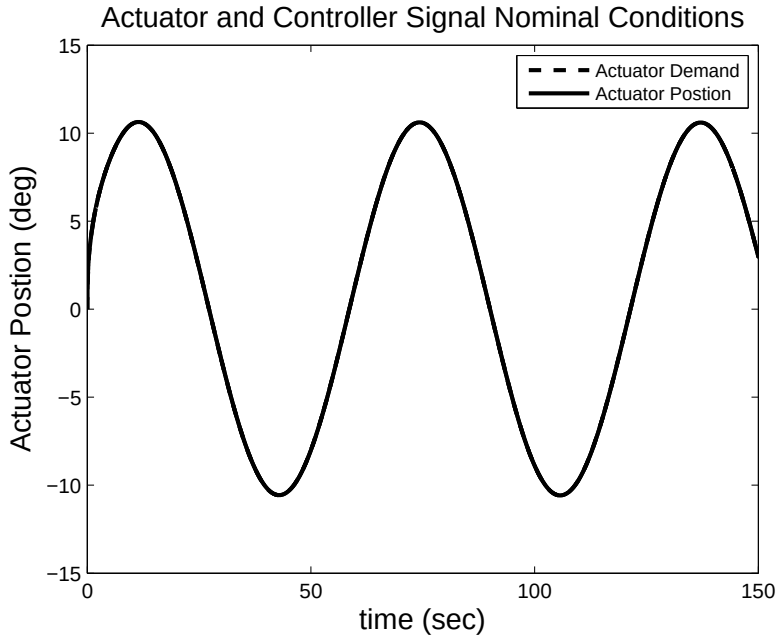

Figure 2.6. Actuator and controller output with no failure.

CHAPTER 3

REFERENCE TRAJECTORY MODIFICATION USING MODEL INVERSION

3.1 System Failures - Saturation

The nominal system shown in the previous chapter is subjected to an actuator failure. The types of failures that will be shown in this thesis will be limited to position saturation failure and parameter drift. With these two types of failures, it is possible to represent a large class of failures that are commonly encountered in practice. To further simulate the actual environment, the severity and time of failure introduced into the system will not be known. The severity of the failure will be such that the system can no longer perform asymptotic tracking of the original reference trajectory, and the persistent excessive excitation by the controller in light of the unanticipated failure may cause system instabilities. These instabilities will be caused by deterioration in the actuator dynamics and response.

Virtually all control actuation devices are subject to magnitude and/or rate limits and this typically leads to degradation of the nominal performance and even to instability. This phenomenon has traditionally been referred to as "windup" [17]. The saturation failure can be modeled as follows: if the signal $\delta_e(t)$ is under the influence of the saturation failure, with a maximum absolute value $\delta_{e_{\max}}$, the saturation can be modeled by:

$$\mathrm{sat}(\delta_e(t)) = \left\{ \begin{array}{cc} \delta_e(t), & \text{if } \delta_e(t) \leq \delta_{e_{\max}} \\ \delta_{e_{\max}} \mathrm{sign}(\delta_e(t)), & \text{if } \delta_e(t) > \delta_{e_{\max}} \end{array} \right\} \tag{3.1}$$

where

$$\text{sign}(u) = \left\{ \begin{array}{ll} 1, & \text{if } u > 0 \\ 0, & \text{if } u = 0 \\ 11, & \text{if } u < 0 \end{array} \right\} \tag{3.2}$$

Note, from Equation 2.3

$$\delta_e(t) = \mathcal{L}^{-1}\left\{\delta_e(s)\right\} = \mathcal{L}^{-1}\left\{\frac{C(s)n_A(s)}{d_A(s)}\right\} \tag{3.3}$$

where, $\mathcal{L}^{-1}$ is the inverse Laplace transform of $u(s)$. Figure 3.1 shows how the system responds to a step input with a position saturation failure occurring at 30 sec. The unexpected saturation changes the saturation point of the actuator from $\pm 70^\circ$ to $\pm 6^\circ$. The effects of the position saturation are clearly evident. The PID controller creates an actuator windup issue that creates a large lag between the controller and the actuator response. This can be clearly seen in Figure 3.2 that shows how the saturated actuator responds to the controller input. As the reference trajectory continues to command step inputs to the system, the resulting controller action continues to increase as well. In addition, the F-16 model is no longer able to obtain the commanded pitch rate of 5 deg/sec. A similar response is observed for a sinusoidal input shown in Figures 3.3 and 3.4.

3.2 Stable Reference Trajectory Modification

The reference trajectory modification is designed to augment nominal reference trajectories to enhance the overall system performance and stability. To achieve the goal of modifying the trajectory in the presence of failure that alter the dynamic characteristics of system components, this method utilizes current system conditions to determine an achievable trajectory without any modification of the nominal closed loop structure of the flight control system. In addition, this modification can be carried out without complex neural network or adaptation routines. Figure 3.5 shows the

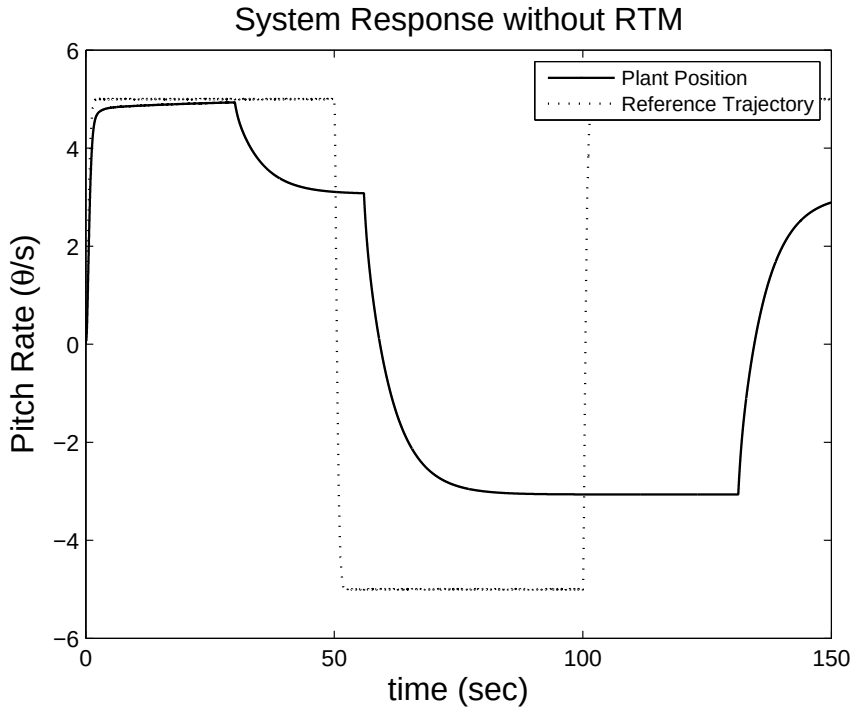

Figure 3.1. System response to $r(t)$; The original step reference trajectory.

general architecture of the RTM. The components required for the method include the following: nominally stable closed loop system, a HMS that examines the condition of major system variables, and real-time trajectory generation for modification.

3.2.1 Health Monitoring System (HMS)

The HMS monitors a large number of both critical and non-critical system components, and serves to detect when system states are going astray. This may be due to some sort of system failure, external disturbances, or inadequate system input. The approach developed in this section utilizes a simplified version of a HMS. The HMS is a key component of the RTM. The goal of this HMS is to determine if the proposed modified trajectory will result in improved system tracking performance over the original reference trajectory. This proposed HMS will also control the update

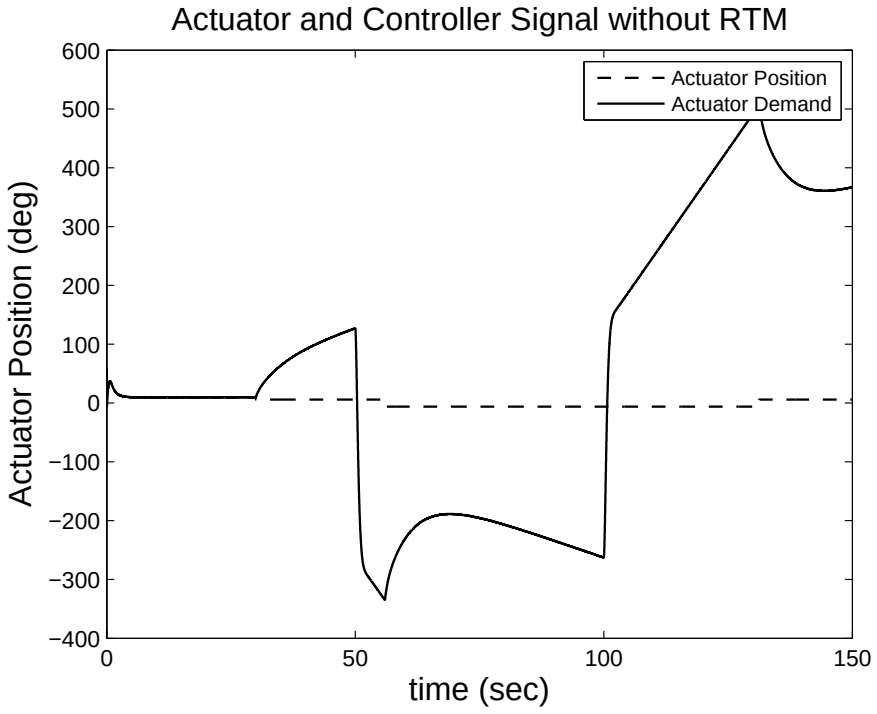

Figure 3.2. Actuator and controller output to the original step reference trajectory $r(t)$.

of the reference trajectory. If the original reference trajectory produces an acceptable level of system performance, then no additional updates are needed to the reference trajectory. An "acceptable system performance" is the acceptable amount of error between the system output and the reference trajectory it is meant to track. As the HMS detects tracking and/or system degradation, the modified trajectory is used. This new trajectory is developed with consideration to the current system. Figure 3.6 depicts a switching criterion which is used by the HMS and computed continuously. The inclusion of the HMS makes this system an intelligent control architecture with the lower level containing ordinary control mechanisms, while the upper level, the HMS, monitors overall progress of the controlled system. The signals and parameters used to evaluate the switching conditions are as follows:

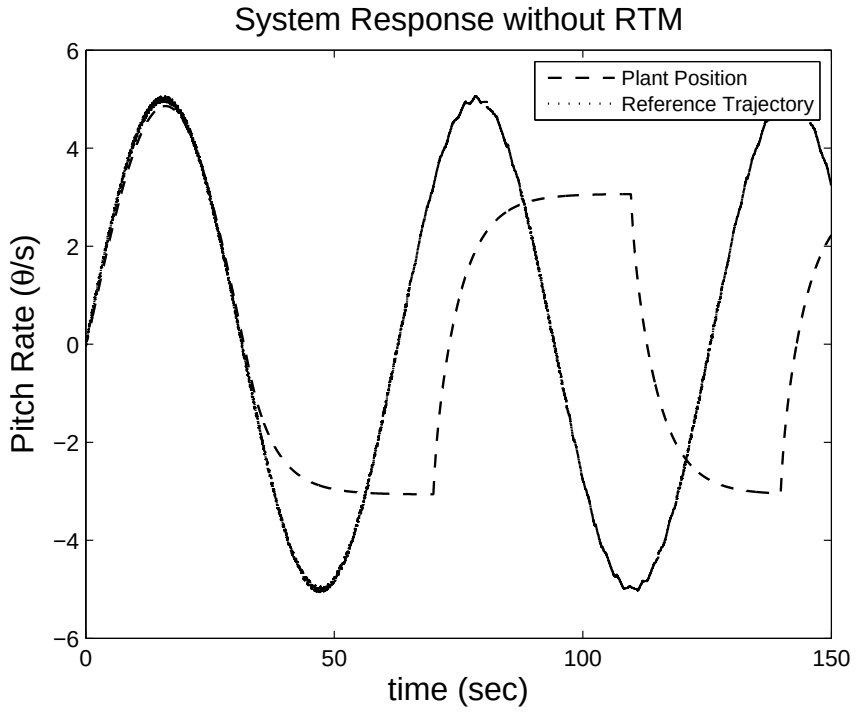

Figure 3.3. Plant response to original trajectory $r(t)$ - The original sinusoid reference trajectory is a Sinusoidal Input.

r	Nominal Trajectory generated by $R(s)$
r_{mod}	Modified trajectory
δ_e	True actuator (elevator) deflection
u_e	Commanded actuator deflection generated by PID controller
Δ_e	The difference between the actual and commanded deflection; $\parallel \delta_e \parallel_2 - \parallel u_e \parallel_2$
ε_{act}	Actuator error threshold

The switching criterion controls the update of the reference trajectory. If degradation in the system performance is detected then a new reference trajectory, based on system states and conditions, is created and tracked. The first block in Figure 3.6

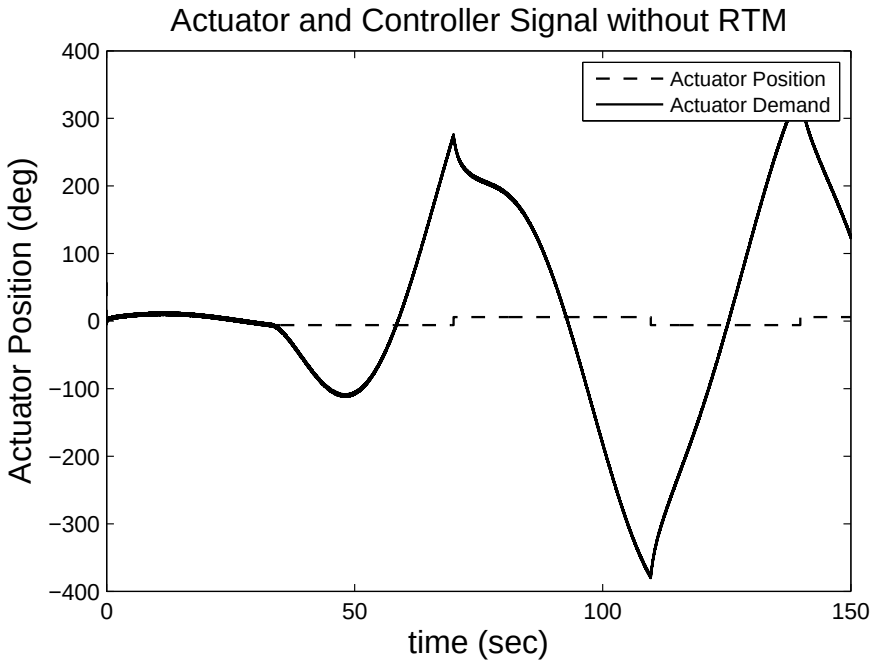

Figure 3.4. Actuator and controller output signal to original sinusoid trajectory $r_{mod}(t)$.

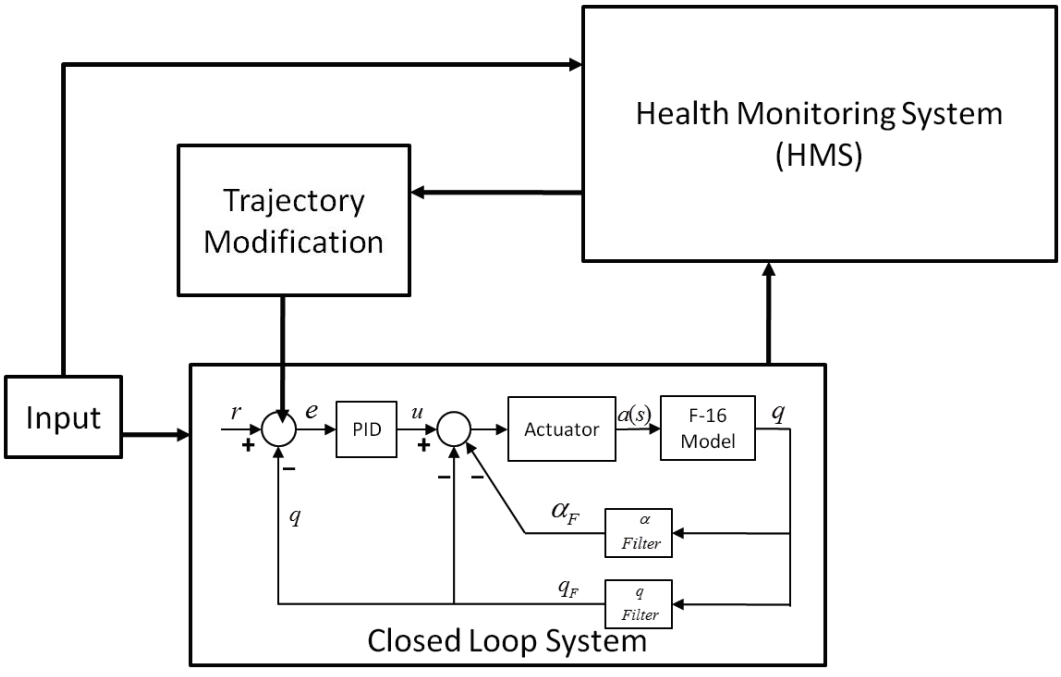

Figure 3.5. Basic overview of system architecture.

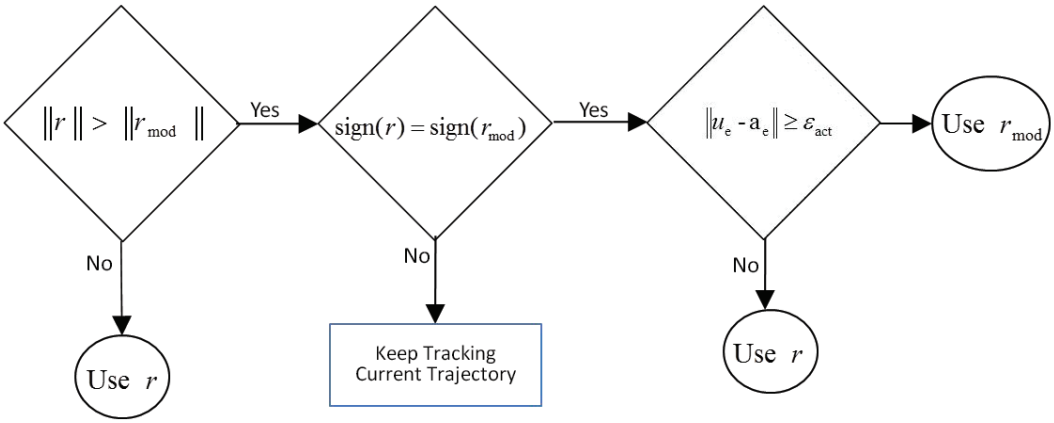

Figure 3.6. Switching Conditions.

compares the signs and norms of the two trajectories. The clear choice at this juncture is to track the original trajectory if its norm is less than the trajectory created from the modification; however, if the modified trajectory's magnitude is less than the nominal trajectory then further information is needed before making a determination to switch to the modified trajectory. The next block considers the states of the actuator, δ_e, and compares it with the commanded value generated by the PID controller, u_e. If $\| u_e \| > \| \delta_e \|$ and the magnitude of this difference is greater than ε_{act}, the actuator error threshold, the system now tracks the modified trajectory. However, if both of these conditions are not met, the system continues to track its previous reference trajectory.

The modification generates $\Delta_r(s)$ from the signals $a(s)$ and $y(s)$ which is used to adjust the original reference trajectory $r(s)$ to accommodate for saturation in the actuator. The result of this is that the plant tracks $r_{mod}(s)$ instead of $r(s)$ which will prevent the adverse effects of saturation. Figure 3.7 shows how the signal $\Delta_r(s)$ is generated where $M(s)$ is the transfer function used to generate $r_a(s)$ from the actuator output $a(s)$. The transfer function $M(s)$ in the upper feedback path is used to update the reference trajectory.

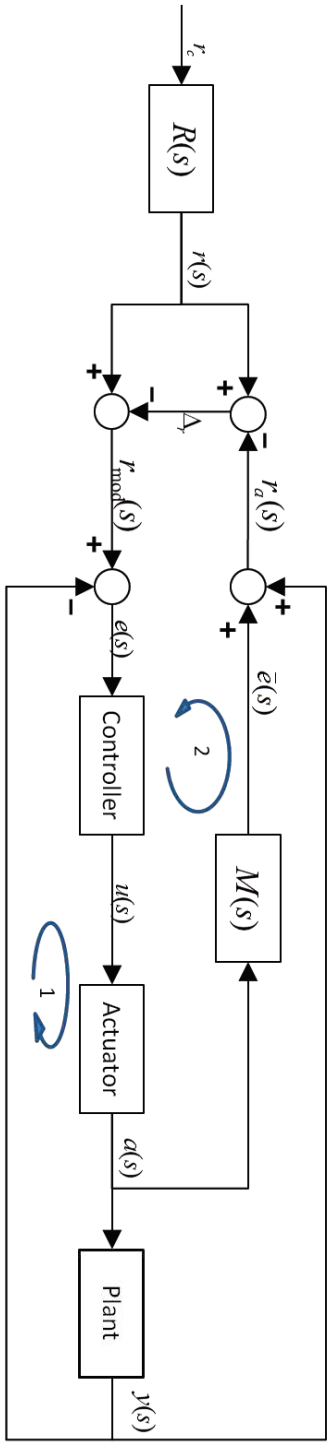

Figure 3.7. Modification feedback loop structure.

The intent of the feedback path is to generate an achievable trajectory $r_a(s)$ based on the real time actuator position. The scheme shown in this block diagram provides some inherent properties that will allow for successful modification of the original reference trajectory. The second loop (2) in this system acts as a monitor that determines how well the system output and the actuator are responding to system inputs and then alters the trajectory accordingly. This loop can be viewed as a parallel system that has identical inputs as the original system while the output is a signal that is used to update the input of the original system. This is possible first by comparing a filtered actuator output with the plant output. The term "filtered" indicates that the signal has been passed through the transfer function $M(s)$. This filtered signal $\bar{e}(s)$ is obtained to ensure that a tractable reference is generated and that the actuator output signal $a(s)$ is adequate and will create desirable results. An adequate actuator output signal is one that first, does not create instabilities due to input or output saturations, and second, is capable of matching the controller demand while the actuator states remain within a desired operating range. This is the role of transfer function $M(s)$. The objective is to obtain a function $M(s)$ that ensures these conditions on $a(s)$. Next the output from the transfer function $M(s)$ and the system output are used to generate a modified trajectory which will no longer saturate the actuator or create wind-up in the integral states of the controller. This ideal trajectory $r_a(s)$ is used to obtain the modified trajectory $r_{mod}(s)$ through a series of summing junctions. The feed forward nature of this system means that the modification scheme is anticipating changes in the reference trajectory and adjusting accordingly. Therefore, the ill effects that may be created by an unsuitable reference trajectory signal are detected and avoided prior to being realized by the original system. All this is monitored by the switching criterion that in essence turns on and off the modification in the system. The following signals can be defined as follows:

$$r_a(s) = y(s) + \bar{e}(s) \tag{3.4}$$

$$\bar{e}(s) = M(s)a(s) \tag{3.5}$$

$$y(s) = P(s)a(s) \tag{3.6}$$

$$a(s) = A(s)C(s)\left(r_{mod}(s) - y(s)\right) \tag{3.7}$$

The first feedback loop in Figure 3.7 was shown in Equation 2.4. The expression for the second loop can be shown by considering the output/input relationship for $r_a(s)$ and $a(s)$ respectively. Using the expressions for $r_a(s)$, $\bar{e}(s)$, and $y(s)$ the following equation is obtained;

$$\frac{r_a(s)}{a(s)} = P(s) + M(s) \tag{3.8}$$

The third loop in Figure 3.7 will be expressed using $\Delta_r(s)$ and $r(s)$ as the output and input respectively. At the summing junction:

$$\Delta_r(s) = r(s) - r_a(s) \tag{3.9}$$

substituting Equation 3.4 and dividing through by $r(s)$

$$\frac{\Delta_r(s)}{r(s)} = 1 - \left[\frac{y(s)}{r(s)} + \frac{\bar{e}(s)}{r(s)}\right] \tag{3.10}$$

By using Equations 3.5, 3.6 and 3.7

$$\Delta_r(s) = r(s) - \left[P(s) + M(s)\right] A(s)C(s)\left[r_{mod}(s) - y(s)\right] \tag{3.11}$$

Noting that $r_{mod}(s) = r(s) - \Delta_r(s)$ Equation 3.11 can be factored into the following equation:

$$\begin{gathered}\left[1 - \left(P(s) + M(s)\right) A(s)C(s)\right]\Delta_r(s) = \\ \left[\left(P(s) + M(s)\right) A(s)C(s)\right] y(s) + \left[1 - \left(P(s) + M(s)\right) A(s)C(s)\right] r(s)\end{gathered} \tag{3.12}$$

This equation can be simplified to

$$\frac{\Delta_r(s)}{r(s)} = 1 + \left[\frac{[P(s)+M(s)]\,A(s)C(s)}{1-[P(s)+M(s)]\,A(s)C(s)}\right]\left(\frac{y(s)}{r(s)}\right) \tag{3.13}$$

Equation 3.13 is the expression showing output/input relationship for the third feedback loop. Another useful relationship to show is the output $y(s)$ to the achievable trajectory $r_a(s)$ that can be found by combining Equation 3.9 with Equation 3.13.

$$\frac{y(s)}{r_a(s)} = -\left[\frac{1-[P(s)+M(s)]\,A(s)C(s)}{[P(s)+M(s)]\,A(s)C(s)}\right] \tag{3.14}$$

3.2.2 Steady State Stability

The purpose of this section is to investigate the closed loop steady state stability of the modification. The stability during saturation and the transient after will not be reflected in these results. The stability during saturation and the transient require nonlinear stability analysis. However, the first step is to ensure that the steady state results will be stable. This can be done with linear stability methods. The trajectory modification loop will be considered since it is already known that the control feedback loop exhibits stable properties by design.

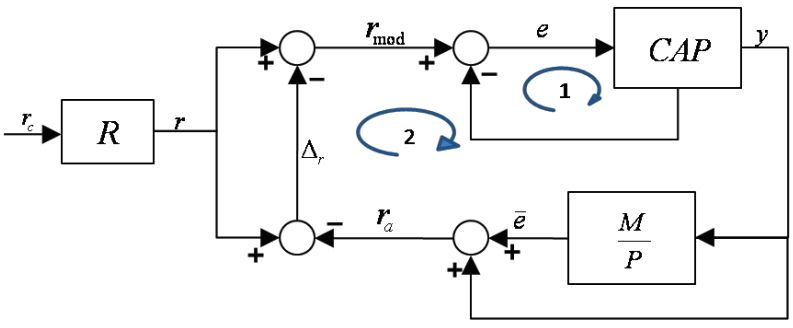

Figure 3.8. Alternate Block Structure.

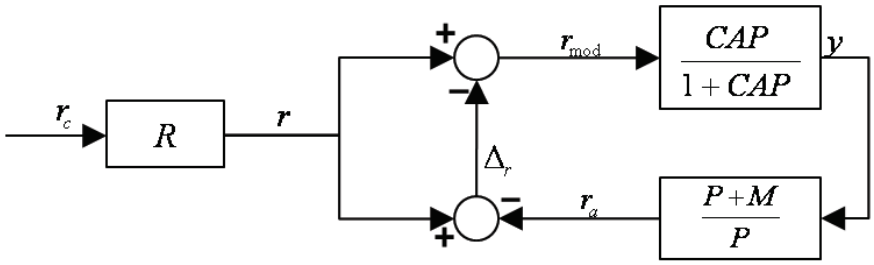

Figure 3.9. System Simplification .

Henceforth the (s) will be omitted from the system variables for brevity. It is implied that all system variables are a function of the Laplace variable s unless otherwise stated. The block structure shown in Figure 3.7 can be simplified to what is shown in Figure 3.8. The input to the modification block is now the plant output. If the plant is known, this can simply be divided out, however, if the plant is not known then some approximate model can be used. Doing this allows the system structure to be simplified, and it clearly shows the inner control feedback loop regulating the plant states and the outer feedback loop modifying the trajectory to ensure it remains achievable. Since the inner loop is stable for all bounded inputs, showing that r_a remains bounded means the system will remain stable. Further simplification of the feedback and feed forward loops in Figure 3.8 produces the result in Figure 3.9.

The transfer function $\frac{P+M}{P}$ must be a proper transfer function and must have bounded-input bounded-output (BIBO) stability properties. A proper transfer function is a transfer function where the degree of the numerator does not exceed the degree of the denominator.

The individual functions M and P maybe written as $\frac{n_M}{d_M}$ and $\frac{n_P}{d_P}$ respectively. Doing so allows the expression to be written as:

$$G = \frac{P + M}{P} = \frac{(n_M d_P + d_M n_P)}{d_M n_P} \tag{3.15}$$

With the transfer function M being a design parameter, the expression for n_M and d_M can be readily chosen to ensure that Equation 3.15 remains proper and has stable properties which will mean the system exhibits steady state stability. To ensure that $\mid G(\pm j\infty) \mid < \infty$ remains true, G must be a proper transfer function. The conditions for which this is true can be determined from Equation 3.15. From this equation, it is clear that the relative degree of M must be greater than the relative degree of P in order for G to be a proper transfer function. Let $M = \lambda M_i$ where $M_i = \dfrac{1}{A_m C}$, and A_m is a model of the actuator. This model can be determined from an estimated or parameterized linear model using the certainty equivalence principle. The transfer function of the controller C is provided by design. Setting M_i in this way guarantees that the signal r_a in Figure 3.9 can be synthesized. Due to the physical nature of the actuator it is apparent that $\dfrac{1}{A_m}$ is an improper transfer function. These are all dynamical systems that are at least first order that have the following form: $f(y_m, y_{m-1}, y_{m-2}, ...y_0) = u$ where, $m \geq 1$. The same will be true of the majority of linear controllers; therefore the transfer function λ is necessary to guarantee that G remains proper. The order of function λ is set such that the two relationships are satisfied.

$$rel(\lambda) - rel(M_i) \geq 0 \tag{3.16}$$

$$rel(\lambda M_i) - rel(P) \geq 0 \tag{3.17}$$

Therefore for any arbitrary plant, actuator, or controller the appropriate order of λ can be determined. For the given plant, actuator, and controller shown in Equation 2.3, in the ideal situation, where one is able to generate reference signal that mimics the output, is a typical model inversion of this kind. This will then lead you to

choose an M of a specific nature which will guarantee that r_a and r_{mod} are identical. However, in the majority of cases this direct approach will not be implementable. A more feasible implementation of these dynamics will be to go through a process where we chose a λ to insure that λM_i is an implementable scheme. For the given transfer function shown in Equation 3.15, if one satisfies these conditions on λ, then it is possible to synthesize a proper M such that the output r_a will ensure that r_{mod} will never generate an a greater than the saturation value, which was created due to system failure.

3.3 Results

The above method was implemented on a second order linear longitudinal F-16 pitch rate system. In all case failure occurs at 30 sec. The figures below show that the algorithm is able to quickly detect the failure and generate a modified reference trajectory for the plant to track. The modified reference trajectory improves system tracking performance.

Figure 3.10 shows how the pitch rate CAS functions with and without RTM. The dashed line shows how the plant responds with no RTM, while solid line is the plant response with RTM. The fault is introduced to the system at 30 secs. Immediately following the actuator fault the plant is no longer capable of maintaining the command pitch rate of 5 deg/sec. However, the original reference continues to hold at the unachievable rate while the modified reference reduces the demand and reacts to current system conditions.

Figure 3.11 shows how the actuator is able to keep up with the requested demands of the PID controller. Figure 3.2 shows how the actuator responded without RTM. The improved actuator response results in a more timely plant response to the changing reference trajectory.

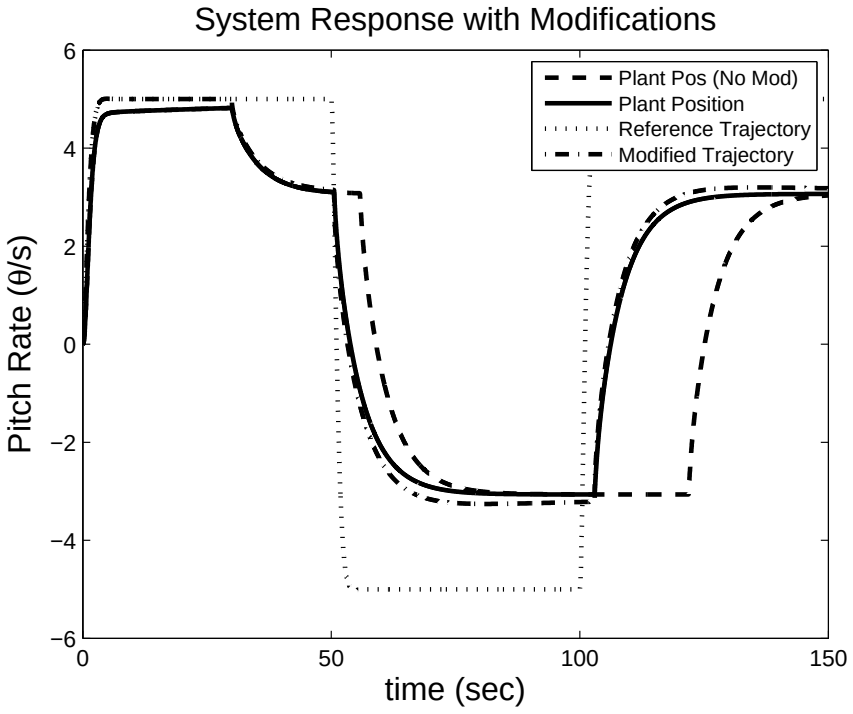

Figure 3.10. Plant response to modified trajectory $r_{mod}(t)$ - The original reference trajectory giving are step inputs.

Figure 3.12 shows how the plant responds to a sine input. Again the dashed line is the plant response without RTM. Once the fault is introduced at 30 sec, the plant is no longer at any point in time able to track the reference trajectory. However, with RTM, the plants tracking of the reference trajectory is much improved. This plot shows that as soon as the demand from the original reference trajectory is within the achievable range of the failed actuator, the modified trajectory converges to match the original reference.

Figure 3.13 shows how the actuator of the system is able to meet the demands of the controller even with an unexpected saturation limit at ± 6 degs. The output from the PID is limited to the capability of the actuator. A quick comparison of Figure 3.13 with Figure 3.4 shows the significant improvement in the actuator response.

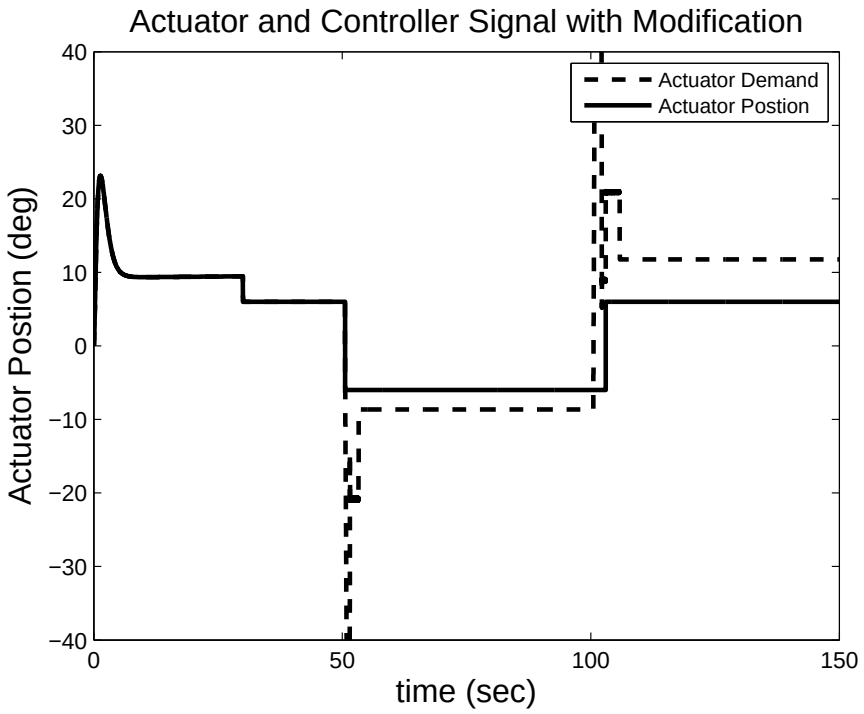

Figure 3.11. Actuator and controller output signal to modified reference $r_{mod}(t)$.

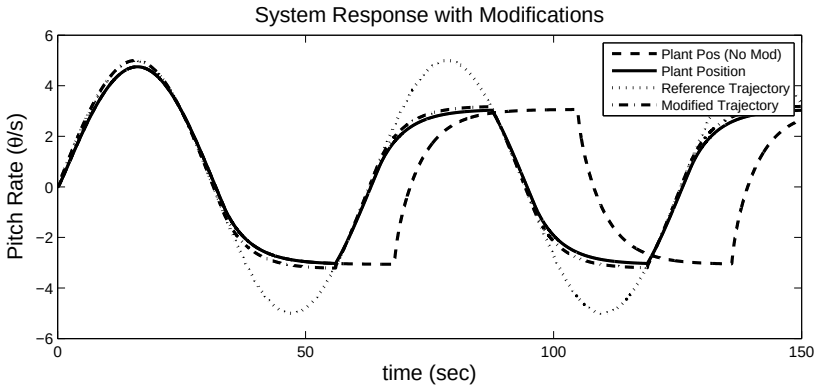

Figure 3.12. Plant response to modified reference $r_{mod}(t)$ - The original reference trajectory giving is a sine wave.

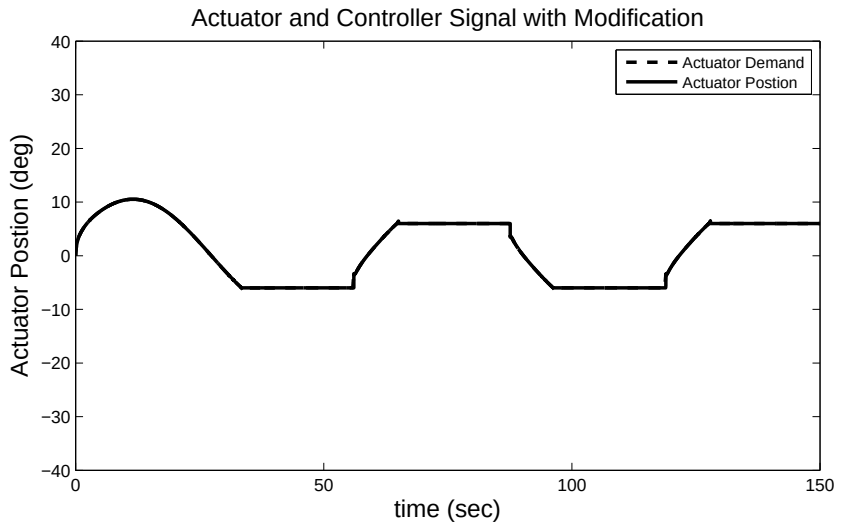

Figure 3.13. Actuator and controller output signal to modified trajectory $r_{mod}(t)$.

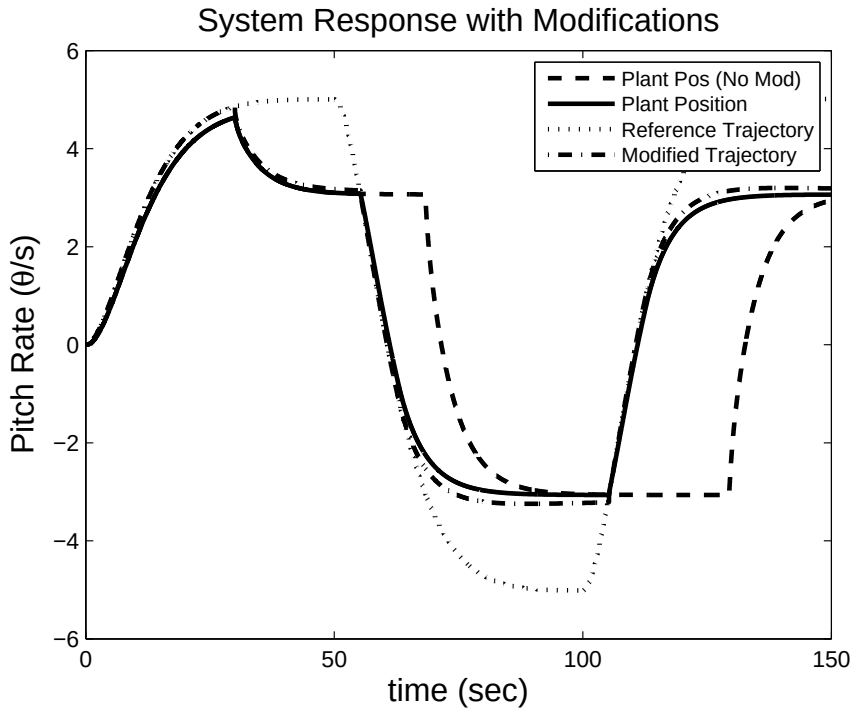

Figure 3.14. System response to modified trajectory $r_{mod}(t)$ - The original reference trajectory are ramp inputs.

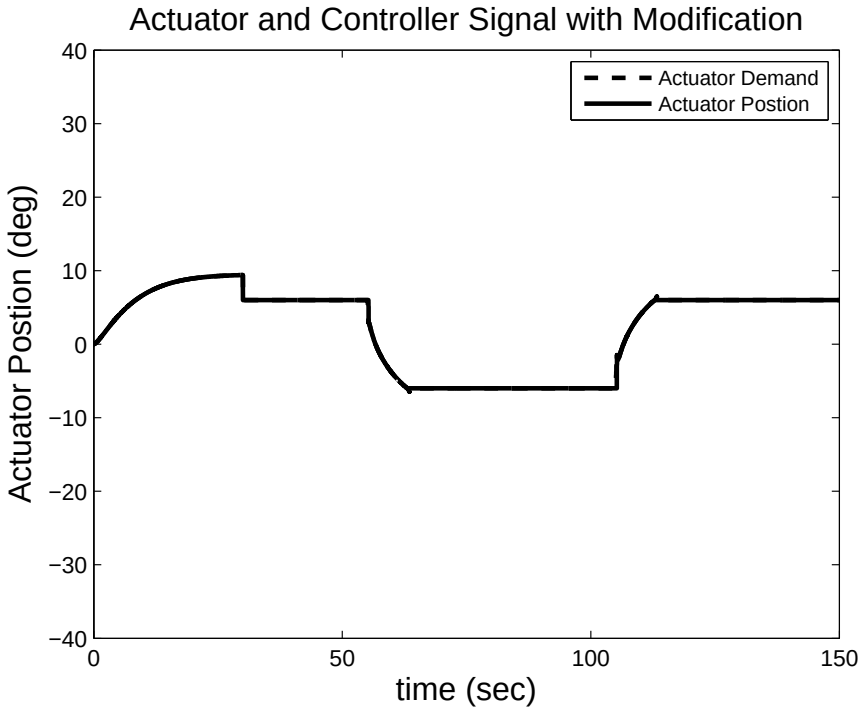

Figure 3.15. Actuator and controller output signal to modified trajectory $r_{mod}(t)$.

A similar improvement is observed in Figure 3.14. The effect of the fault occurring at 30 secs is experienced immediately. The saturation causes a loss in control authority that results in the plant's trajectory to drift away from the original reference. The effect of the saturation continues to grow the tracking error over time. The solid line in Figure 3.14 shows how RTM permits the plant to track the original reference for certain segments of the trajectory.

Figure 3.15 is similar to Figure 3.13. The controller is prevented from overdriving the actuator due to RTM. The plot shows that the actuator is able to effectively operate right at the saturation threshold in spite of the fact that this point is initially unknown by the system, and is a result of an unexpected fault in the actuator. The horizontal portions of Figure 3.15 indicate areas where the full authority of the actuator is requested by the controller.

CHAPTER 4

REFERENCE TRAJECTORY MODIFICATION USING MODEL INVERSION AND AN EXTENDED KALMAN FILTER

4.1 Stable Reference Trajectory Modification (RTM) with EKF

In addition to the HMS, an EKF is used to determine system states. In order to determine a reference trajectory that fully considers real-time operating conditions, the current system parameters must be known. The nominal system parameters maybe known initially, but if the system undergoes some sort of failure that alters the nominal parameters of the system, an EKF will be needed for real-time parameter identification that will increase the robustness of the RTM. The following sections show how the EKF implementation is executed.

4.1.1 System Failures - Parameter Drift

Another failure that will be introduced to the system is parameter drift. This will simulate a loss of bandwidth in the actuator. The actuator model can be represented as follows:

$$\begin{aligned} \dot{\mathbf{x}}_\mathbf{a} &= \mathbf{f}_\mathbf{a}(\mathbf{x}_\mathbf{a}, \mathbf{u}_\mathbf{c}; \mathbf{p}_\mathbf{a}) \\ \mathbf{y}_\mathbf{a} &= \mathbf{h}(\mathbf{x}) \end{aligned} \tag{4.1}$$

where, $\mathbf{x}_\mathbf{a} \in \mathbb{R}^{n_a}$, $\mathbf{p}_\mathbf{a} \in \mathbb{R}^m$, $\mathbf{u}_\mathbf{c} \in \mathbb{R}^s$ represents the actuator's states, actuator's system parameters, and controller command, respectively, and $\mathbf{f} \in \mathbb{R}^{n_a \times 1}$ is a vector function describing the actuator dynamics. The actuator is assumed to undergo failure such that the system parameters drift. In doing so the actuator model now becomes a time varying system that is shown in Equation 4.2. The failed parameters which will be considered in this thesis are the damping ratio ζ and the natural frequency ω_n.

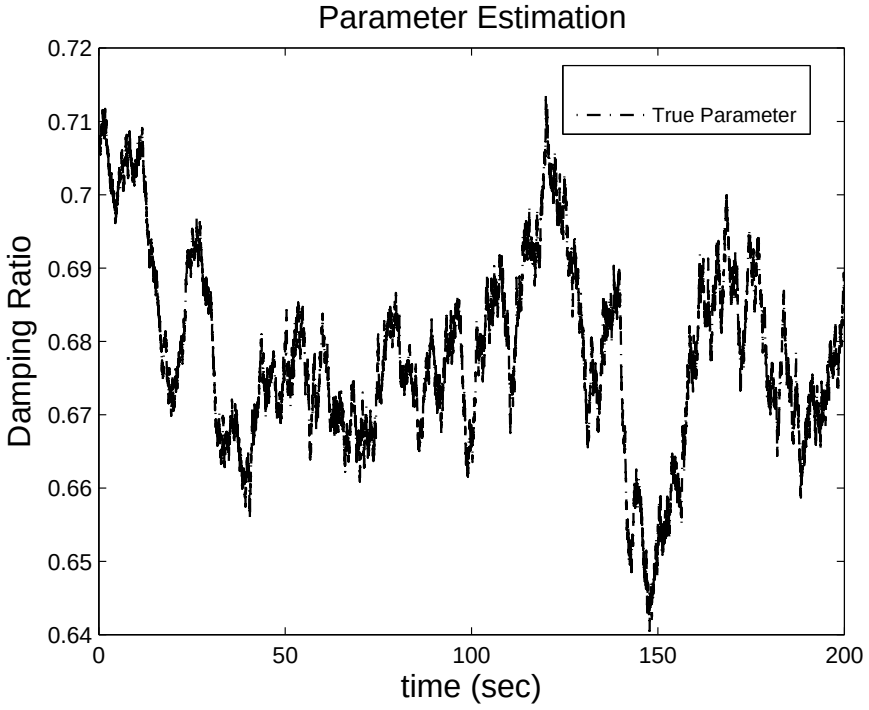

Figure 4.1. The damping ratio ζ is subject to slight random variation during the simulation.

$$\dot{\mathbf{x}}_{\mathbf{af}} = \mathbf{f}(\mathbf{x}_{\mathbf{af}}, \mathbf{p}_{\mathbf{af}}, \mathbf{u}_{\mathbf{c}}, t), \forall t \geq 0 \tag{4.2}$$

and,

$$\mathbf{p}_{\mathbf{af}}(t) = \begin{bmatrix} \omega_{nf}(t) \\ \zeta_f(t) \end{bmatrix} \tag{4.3}$$

where the subscript f indicates post failure conditions. This failed actuator contains unknown time varying parameters $\mathbf{p}_{\mathbf{af}}(t)$ which must be estimated for the modified trajectory. Figures 4.1 and 4.2 show how the parameters will be varied. Figure 4.2 shows a significant reduction in the actuators natural frequency. This variation will be unknown to the system, and therefore, will need online estimation.

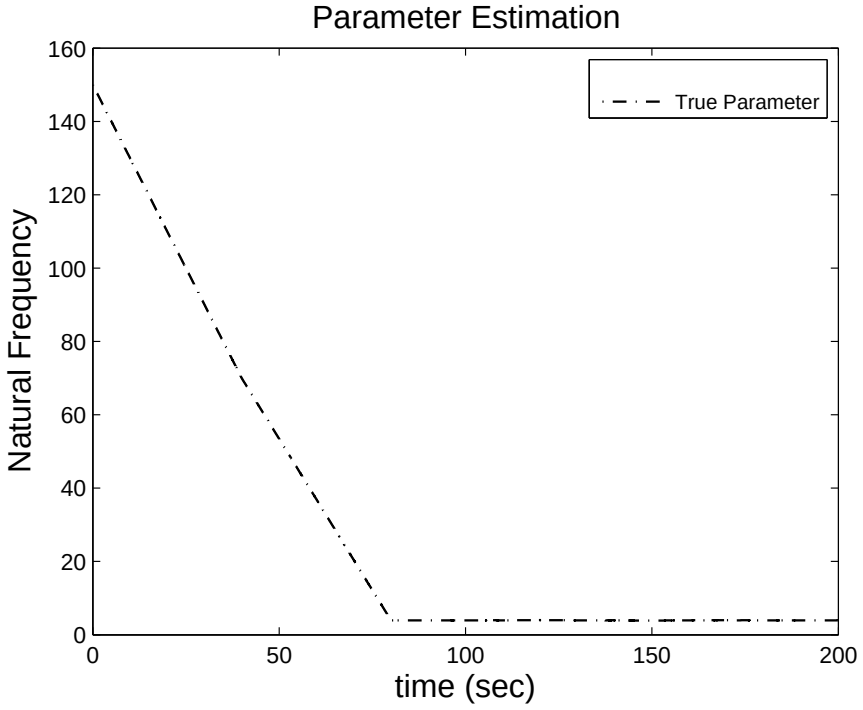

Figure 4.2. The natural frequency ω_n undergoes failure which causes the actuator to lose bandwidth.

The effects of varying the natural frequency and damping ratio parameters for a second order actuator can be observed in Figures 4.3 and 4.4. This shows that large oscillatory responses are introduced into the system.

No information is assumed to be known about the functions $\mathbf{p_{af}}(t)$. Since the variation of the system is not known beforehand, a gain scheduling reconfigurable control law approach cannot be pre-computed, stored, and used to accommodate this real-time failure. The post-failure condition of the system must be detected and identified in real-time. In order to accomplish this, an EKF is proposed to identify the post failure conditions of the actuator system parameters. The goal of the EKF is to obtain an estimate of the system's state based on available measurements. The EKF can easily be developed by treating all unknown actuator parameters as additional states of the original actuator model. In doing so, the augmented state vector is a

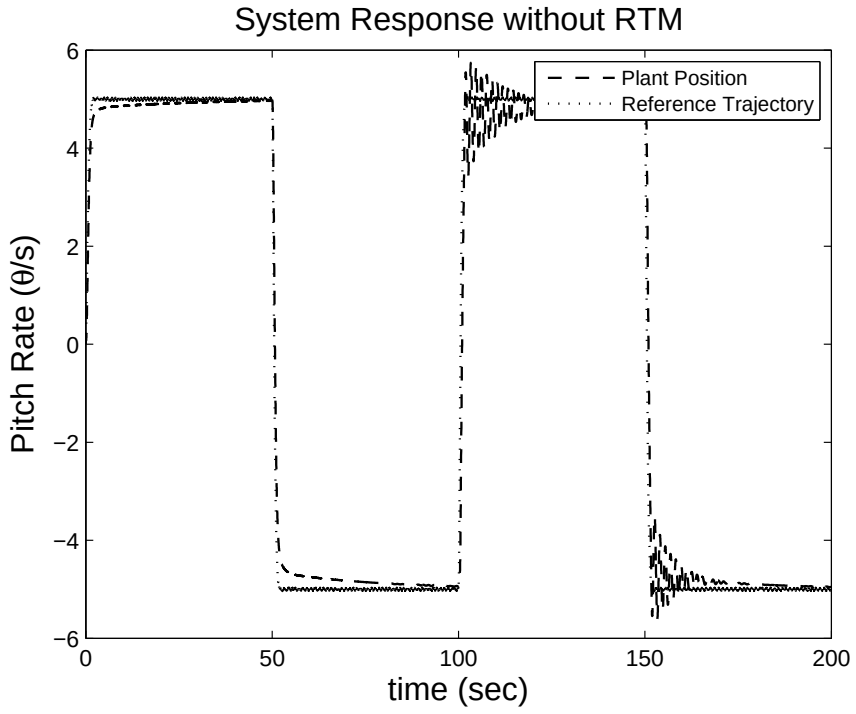

Figure 4.3. The system response to original trajectory r with failed parameters; $\mathbf{p_{af}}(t)$ - The original reference trajectory is a series of step inputs.

combination of the original actuator states and the unknown parameters. The new actuator variables are shown in Equation 4.4;

$$\mathbf{x_A} = \left\{ \begin{array}{c} \mathbf{x_a} \\ \\ \mathbf{p_{af}} \end{array} \right\} \tag{4.4}$$

and the corresponding actuator model can be expressed by

$$\begin{aligned} \dot{\mathbf{x}}_\mathbf{A} &= \mathbf{f_A}(\mathbf{x_A}, \mathbf{u_c}) \\ \mathbf{y_A} &= \mathbf{h_A}(\mathbf{x_A}) \end{aligned} \tag{4.5}$$

where $\mathbf{x_A} \in \mathbb{R}^{n_a+m}$ and $\mathbf{f_A} \in \mathbb{R}^{(n_a+m)\times 1}$ is a vector function. The EKF is implemented following the routine obtained from [18]. The EKF gives an approximation of the optimal state estimate. The non-linearities of the system's dynamics are approximated by a Taylor series expansion to obtain a linearized version of the non-linear system

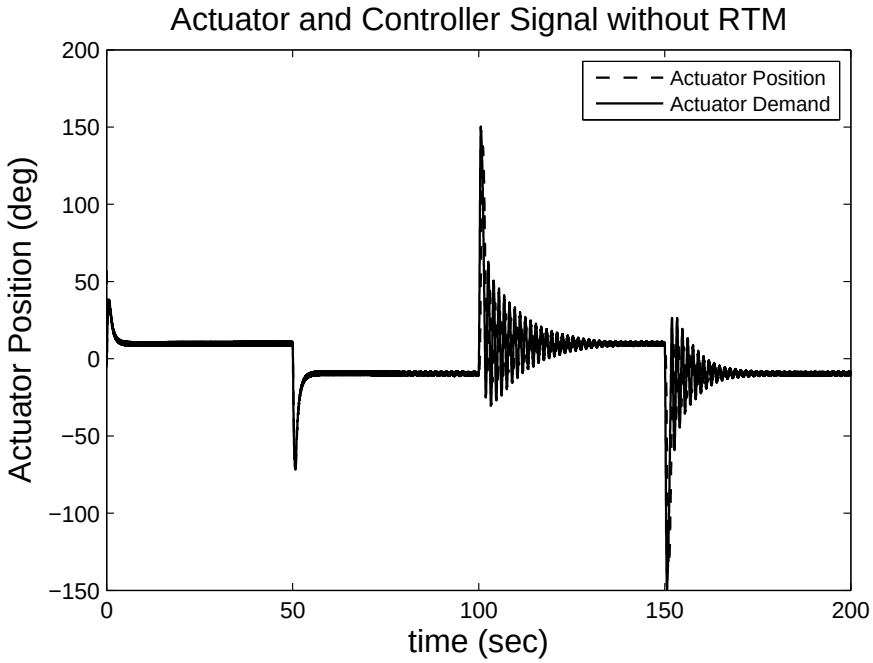

Figure 4.4. The actuator and controller response to the original trajectory r with failed parameters; $\mathbf{p_{af}}(t)$.

around the last state estimate. For this approximation to be valid, this linearization should be a good approximation of the non-linear model in all the uncertainty domains associated with the state estimate. This is how the covariance matrix $P(t)$ is populated [18]. It is worth noting that the EKF is not an optimal estimation and the filter may diverge if the continuously computed linearizations are not a good approximation of the non-linear model in all the associated uncertainty domain. Equation 4.6 shows the formulation that was used for the EKF. A high frequency low amplitude signal is added in order to dither the system, which improves the accuracy of the EKF. The output of the EKF generates the set of estimated parameters $\hat{\mathbf{p}}_{\mathbf{at}}(t)$.

Model

$$\begin{aligned} \dot{\mathbf{x}}_{\mathbf{A}} &= \mathbf{f}_{\mathbf{A}}(\mathbf{x}_{\mathbf{A}}, \mathbf{u}_{\mathbf{c}}) + G(t)\mathbf{w}(t), \mathbf{w}(t)\ N(\mathbf{0}, Q(t)) \\ \mathbf{y}_{\mathbf{A}} &= \mathbf{h}_{\mathbf{A}}(\mathbf{x}_{\mathbf{A}}) + \mathbf{v}(t), \mathbf{v}(t)\ N(\mathbf{0}, Q(t)) \end{aligned} \tag{4.6}$$

Initialization

$$\begin{aligned} \hat{\mathbf{x}}_{\mathbf{A}}(t_0) &= \hat{\mathbf{x}}_{\mathbf{A0}} \\ P_0 &= E\left\{\tilde{\mathbf{x}}_{\mathbf{A}}(t_0)\tilde{\mathbf{x}}_{\mathbf{A}}^{\mathbf{T}}(t_0)\right\} \end{aligned} \tag{4.7}$$

Gain

$$K(t) = P(t)H^T(\hat{\mathbf{x}}_{\mathbf{A}}(t), t)R^{-1}(t) \tag{4.8}$$

Covariance

$$\dot{P}(t) = F(\hat{\mathbf{x}}_{\mathbf{A}}(t), t)P(t) + F^T(\hat{\mathbf{x}}_{\mathbf{A}}(t), t) - P(t)H^T(\hat{\mathbf{x}}_{\mathbf{A}}(t), t)R^{-1}H(\hat{\mathbf{x}}_{\mathbf{A}}(t), t)P(t) \tag{4.9}$$

where,

$$\begin{aligned} F(\hat{\mathbf{x}}_{\mathbf{A}}(t), t) &\equiv \tfrac{\partial \mathbf{f}}{\partial \mathbf{x}_A} \mid_{\hat{\mathbf{x}}_{\mathbf{A}}(t)} \\ H(\hat{\mathbf{x}}_{\mathbf{A}}(t), t) &\equiv \tfrac{\partial \mathbf{f}}{\partial \mathbf{x}_A} \mid_{\hat{\mathbf{x}}_{\mathbf{A}}(t)} \end{aligned} \tag{4.10}$$

Estimate

$$\dot{\hat{\mathbf{x}}}_A = \mathbf{f}(\hat{\mathbf{x}}_{\mathbf{A}}(t), \mathbf{u}(t), t) + K(t)[\tilde{\mathbf{y}}(t) - \mathbf{h}(\hat{\mathbf{x}}_{\mathbf{A}}(t), t)] \tag{4.11}$$

4.2 Modification

Under nominal conditions the reference trajectory r, and the PID gains, are originally designed assuming an actuator model shown in Equation 2.3, which results in a nominal system output, y. Now the actuator undergoes failure that causes premature saturation, or the parameters to become time dependent that compromises the performance of the system. Therefore, the post-failure error signal e_f is now providing inputs to the system that can cause instabilities, or other undesired responses. In order to prevent this from occurring, the system must be adapted in such a way that after the failure takes place the reference command must account for the unexpected system changes.

One approach is to add an additional signal Δ_r prior to the summation junction where e is generated such that the new reference signal r_{mod} is now within the allowed

range of the system. As detailed in a previous chapter, the modification is carried out using a type of model inversion. The transfer function $M(s)$ is used to generate the reference trajectory. $M(s)$ consist of an inverted model of the actuator and controller filtered by a function $\lambda(s)$.

$$M(s) = \lambda(s)(1/(C(s)A(s)) = \lambda(s)(M_0(s)) \tag{4.12}$$

It has been shown that with the proper constraints on the transfer function $\lambda(s)$, Equation 4.12 yields a stable reconfiguration of the reference trajectory. The required order of the function λ is set by the two relationships shown in Equation 3.16 and 3.17. If these constraints are met, then it is possible to generate a proper $M(s)$ such that the resulting modified reference trajectory will improve the tracking performance of the system.

However, due to the time varying nature of the actuator that resulted from system failures, the transfer function $M_0(s)$ is no longer time invariant, nor does the modified trajectory fully account for the real-time system conditions. $M_0(s)$ must be reformed using the output from the EKF to account for varying actuator parameters. Due to the time dependency, M_0 and M are written as time variant transfer functions.

$$\mathbf{M_{0_t}} = \hat{A}_t^{-1}(s)C^{-1}(s) \tag{4.13}$$

$$\mathbf{M_t}(t) = \lambda(s)\hat{A}_t^{-1}(s)C^{-1}(s) \tag{4.14}$$

This function, which is used to generate the modified trajectory is now dependent on the output from the EKF by the term $\hat{\mathbf{p}}(t)$. Once the modified trajectory is generated it is not fed directly to the closed loop system. This is due to the fact that the EKF may incorrectly converge to the actuator parameters, or may even be an

unstable estimation. Due to this, the modified trajectory is sent to the HMS to ensure that the modified trajectory that has been generated, with the EKF parameters, will produce a desirable plant response.

4.3 Results

This method is implemented on a second order linear longitudinal F-16 pitch rate system. The transfer function for the plant is shown in ref [16]. In all saturation cases, the failure occurs at 30 sec. For the parameter drift failure scenarios, the results from the EKF is shown along with other system variables. The EKF is able to estimate the changing system parameters and feeds this information to the HMS, which in turn generates the modified trajectory based on these estimates. The figures below show that the algorithm is able to quickly detect the failure and generate a modified reference trajectory for the plant to track. The modified reference trajectory improves system tracking performance.

The first set of plots show how this algorithm enables the system to accommodate saturation failures. The general method has been shown to respond adequately in [12]. However, the approach discussed in this thesis now includes a HMS and also an EKF, which results in a more complex generation of the modified trajectory.

Figure 4.5 shows how the system responds to a series of step inputs with a position saturation failure occurring at 30 sec. Figure 4.5 also shows how the modified trajectory improves system performance. Though the commanded pitch rate still cannot be reached, the system is much more responsive to commanded inputs. Figure 4.6 shows the much improved actuator and controller performance. Due to the RTM, the controller no longer over-drives the actuator, which results in a more responsive system.

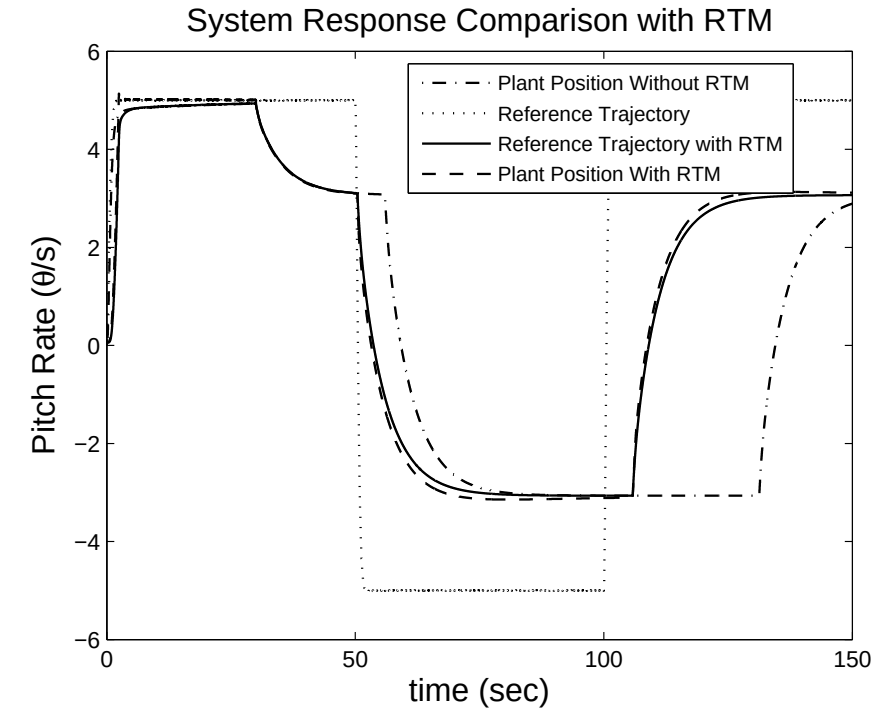

Figure 4.5. Plant response to r_{mod}.

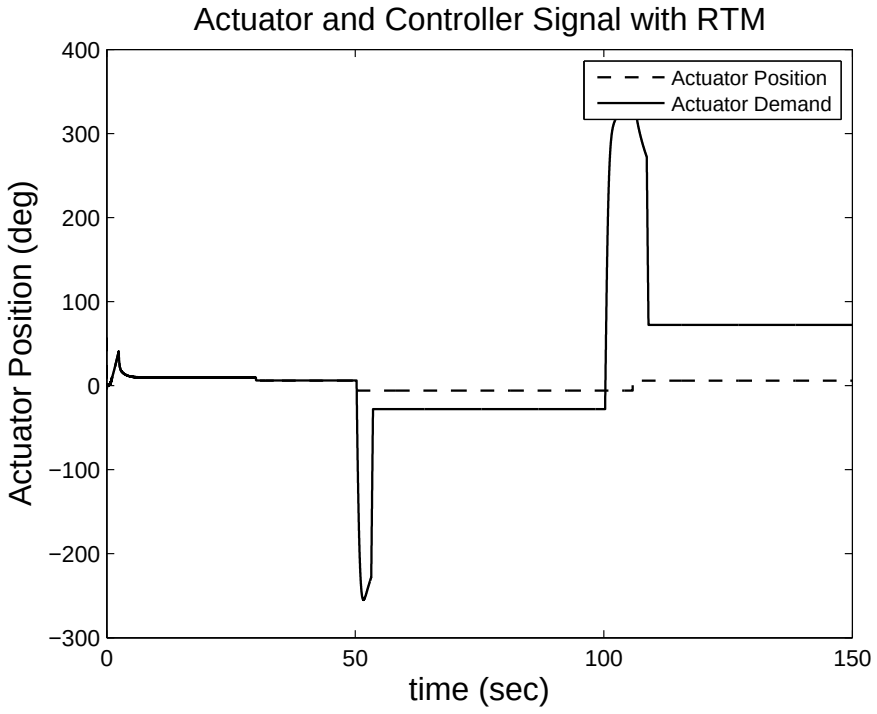

Figure 4.6. Actuator and controller response to modified trajectory r_{mod}.

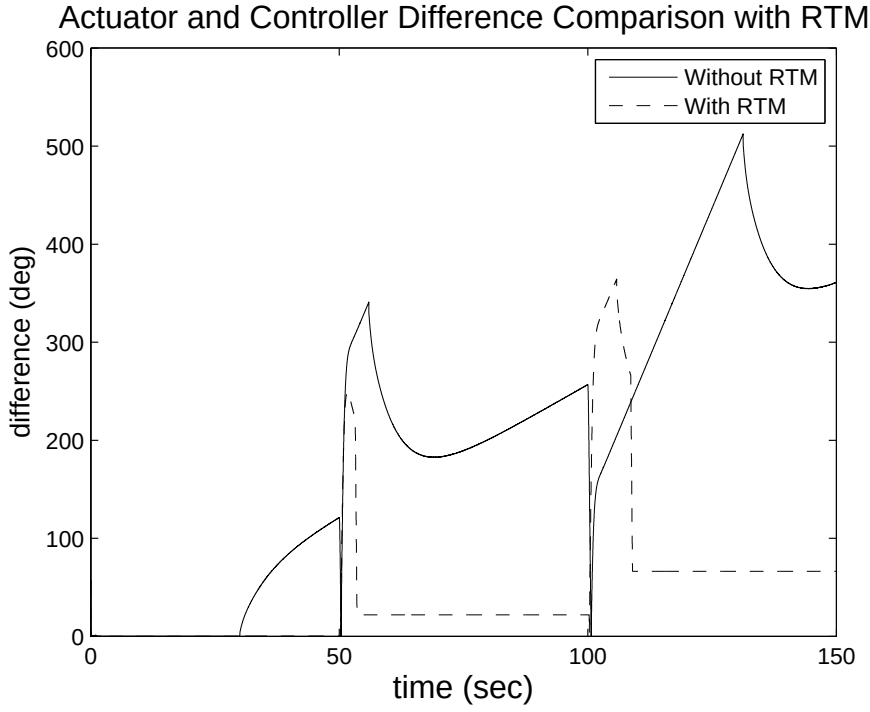

Figure 4.7. Error between the commanded signal u_c and the actuator response δ_c with and without RTM.

Figure 4.7 shows the comparison of two plots. The first plot is the solid line which shows the absolute value of the difference between the controller and the actuator outputs without RTM ($\parallel u_c - \delta_e \parallel$ where u_c is the input to the controller and δ_e is the output of the actuator). The dashed line is the absolute value of the difference between the controller and the actuator outputs with RTM ($\parallel u_{c_{mod}} - \delta_{e_{mod}} \parallel$). This plot shows how the RTM compensates for the failed actuator by reducing the actuator demand.

A similar result can be seen in Figures 4.8 and 4.9. These Figures show how the systems tracks a sine input with and without RTM. The dash-dot is a plot of how the system operates without RTM and under the effects of a saturation failure. Again, the delayed responses of the system output is observed. The dashed and the solid lines show the plant output and the modified reference respectively. This plot

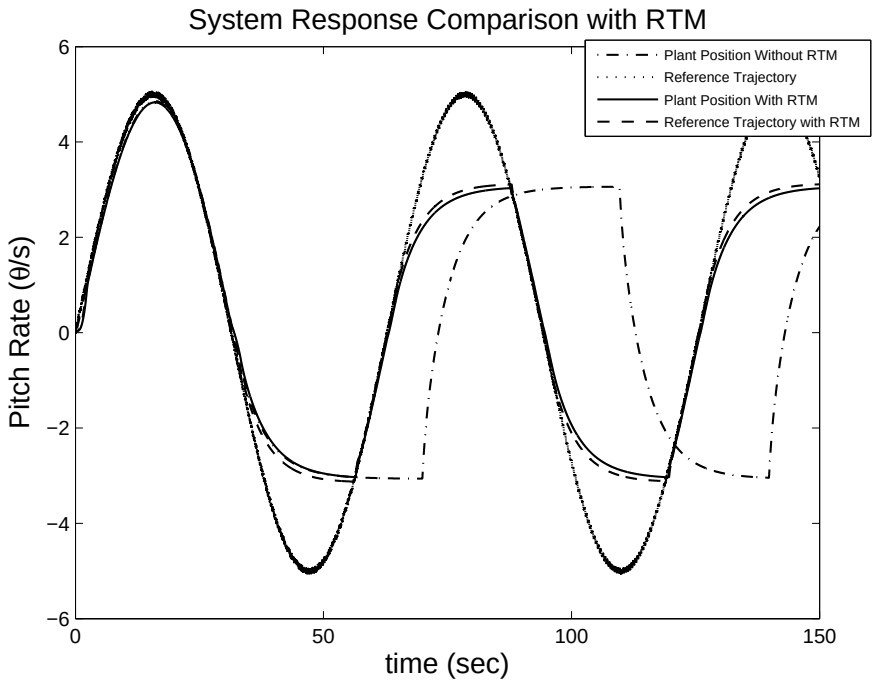

Figure 4.8. Plant response to r_{mod}.

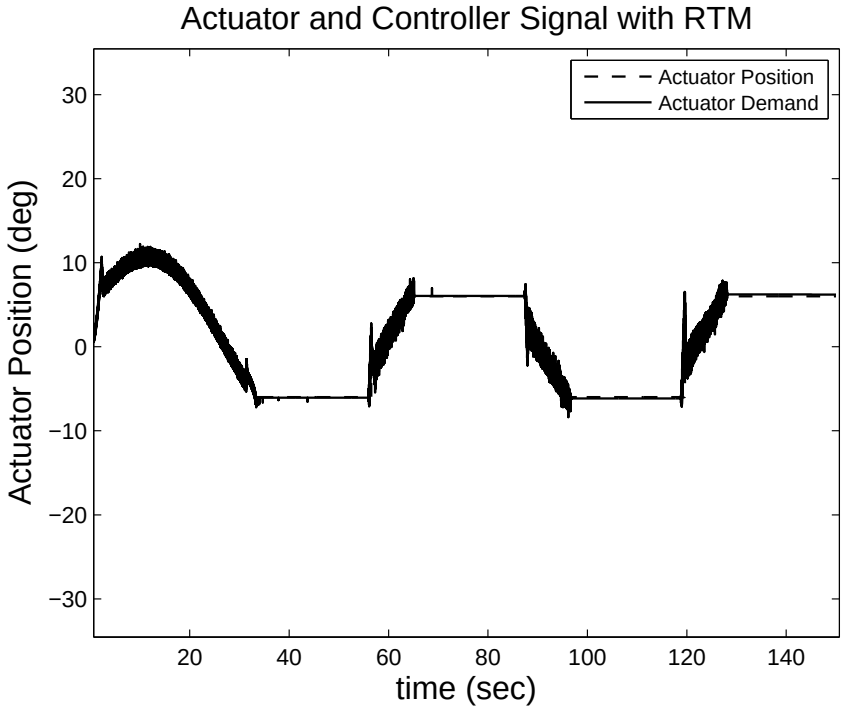

Figure 4.9. Actuator and controller response to modified trajectory r_{mod}.

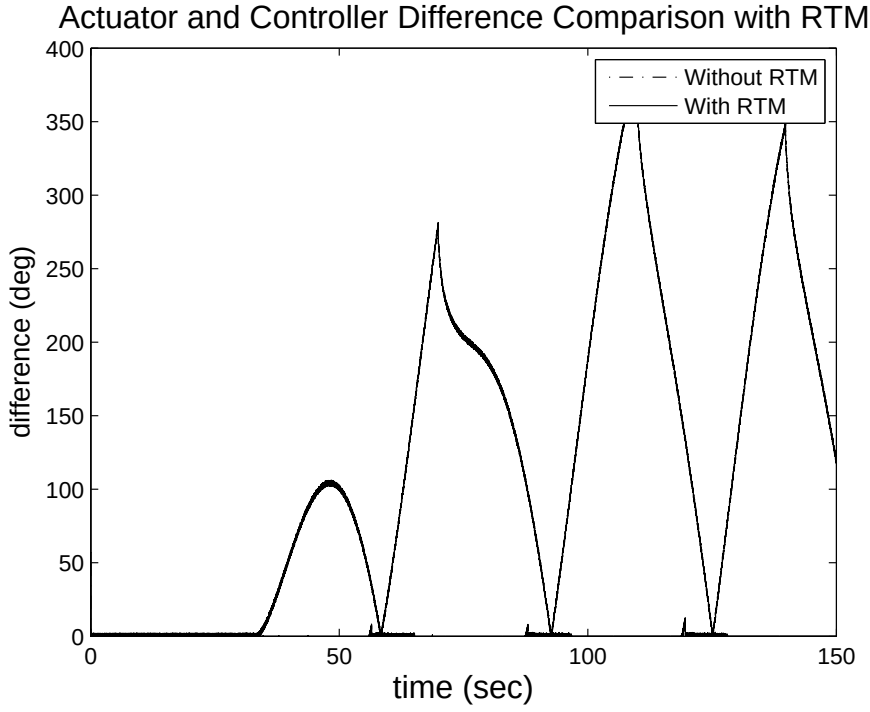

Figure 4.10. Error between the commanded signal u_c and the actuator response δ_c with and without RTM.

shows that asymptotic tracking is still achievable to the modified reference that better mimics the original reference trajectory than the plant output without RTM.

The next set of plots will show how the system handles the parameter drift failure. The assumed failures are shown in Figures 4.1 and 4.2. Figure 4.11 and 4.12 shows how the EKF is able to track the deteriorating actuator parameters. The results for $\hat{\zeta}_f(t)$ are shown in Figure 4.12. This plot reveals that there are periods in which the EKF fails to accurately estimate the parameter $\hat{\zeta}_f(t)$. However, even during the periods of poor estimates of $\hat{\zeta}_f(t)$, this RTM still improved the tracking performance of the plant. The estimates for ω_a are shown in Figure 4.11. This parameter is estimated accurately by the EKF. As the natural frequency drops, the estimate is able to track the loss in bandwidth and feed the updates to the HMS for the reference modification.

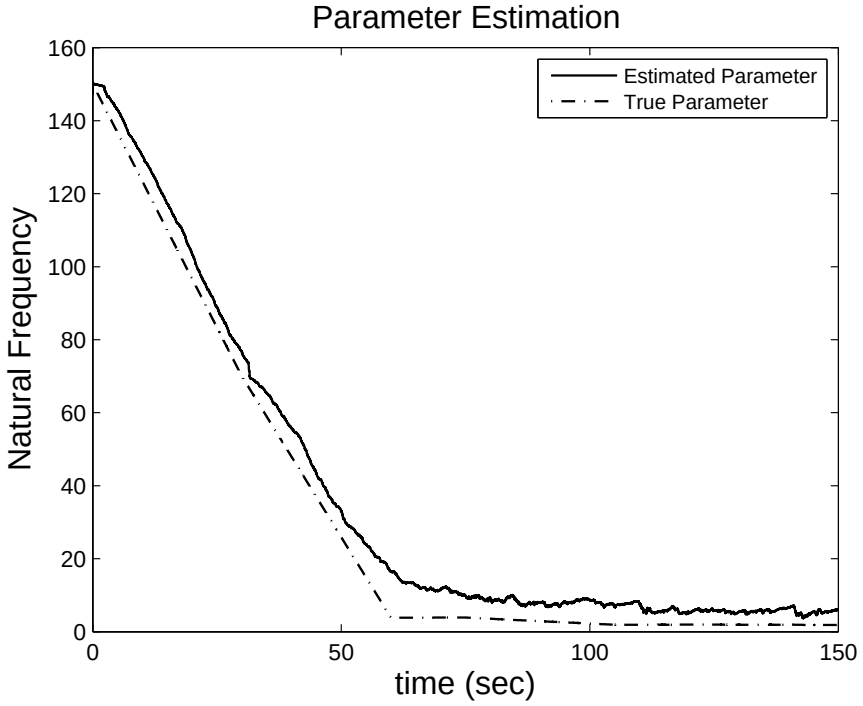

Figure 4.11. The natural frequency ω_n undergoes failure and is tracked by the onboard EKF.

Figures 4.14, 4.14, 4.15, and 4.15, show the plant and actuator responds to a step and sinusoidal input while experiencing parameter drift failure. The large oscillatory behaviour observed is significantly reduced due to the plant now tracking the modified trajectory.

Figures 4.13 and 4.14 show the plant's response to a step input while the actuator experiences parameter drift. In Figure 4.13 the dashed line shows the response to the step input without RTM. Here, the plant now is unable to hold at a pitch rate of 5 degs/sec due to the loss of bandwidth in the actuator. However, with RTM the plants settling time is significantly reduced.

Figure 4.15 and 4.16 show the plants response to a sinusoidal reference trajectory. This relatively modest trajectory induces large oscillations in the pitch rate without RTM. However, with RTM the plant is able to track the reference trajectory

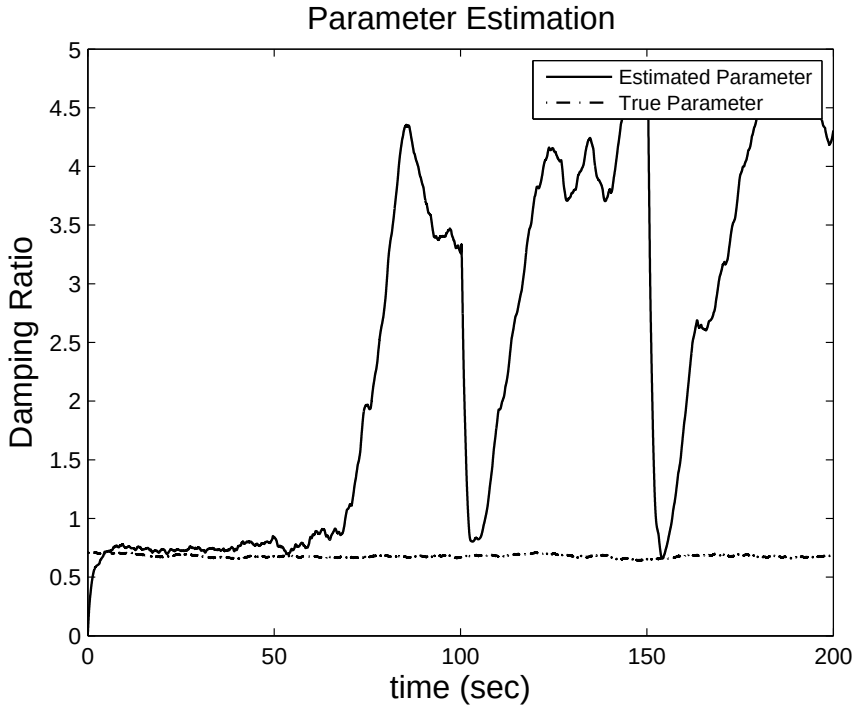

Figure 4.12. The damping ratio ζ_f undergoes failure and to tracked by the onboard EKF.

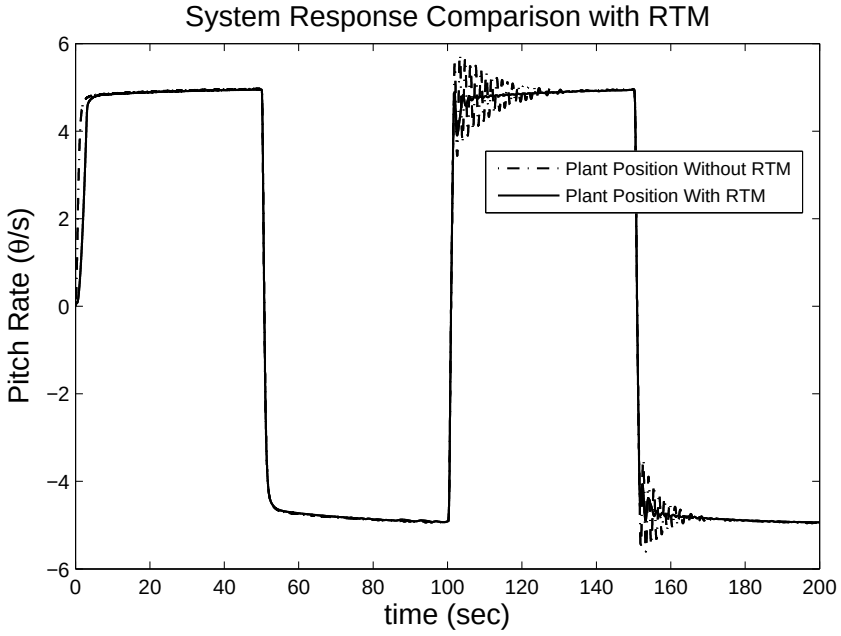

Figure 4.13. Plant response to r_{mod}.

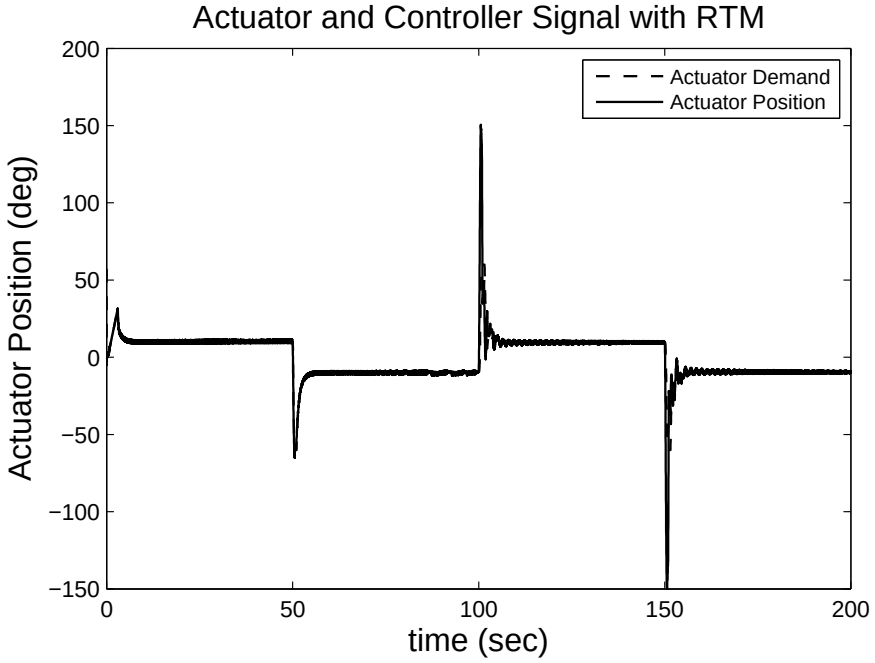

Figure 4.14. Actuator and controller response to modified trajectory r_{mod}.

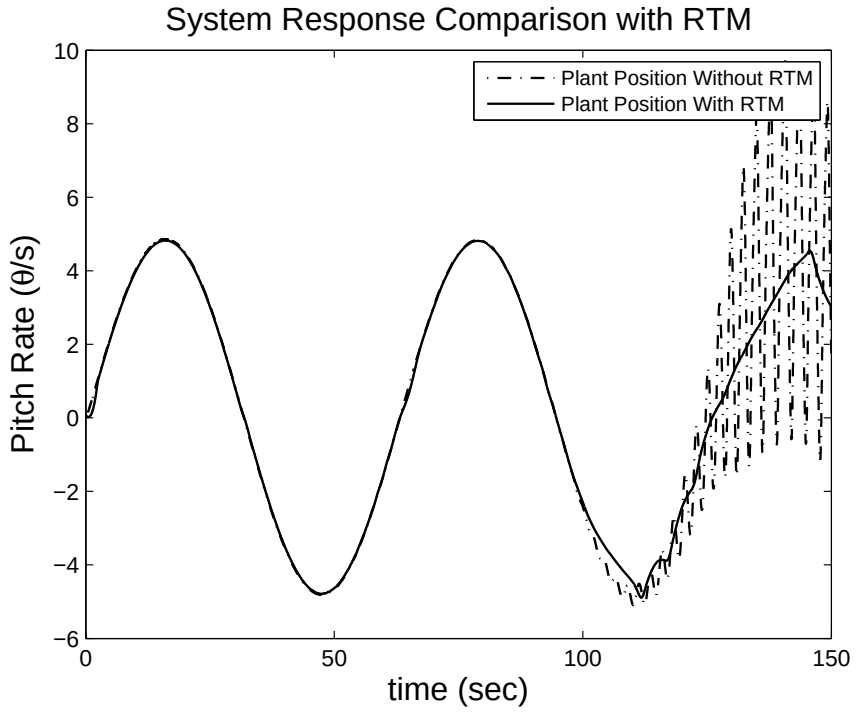

Figure 4.15. Plant response to r_{mod}.

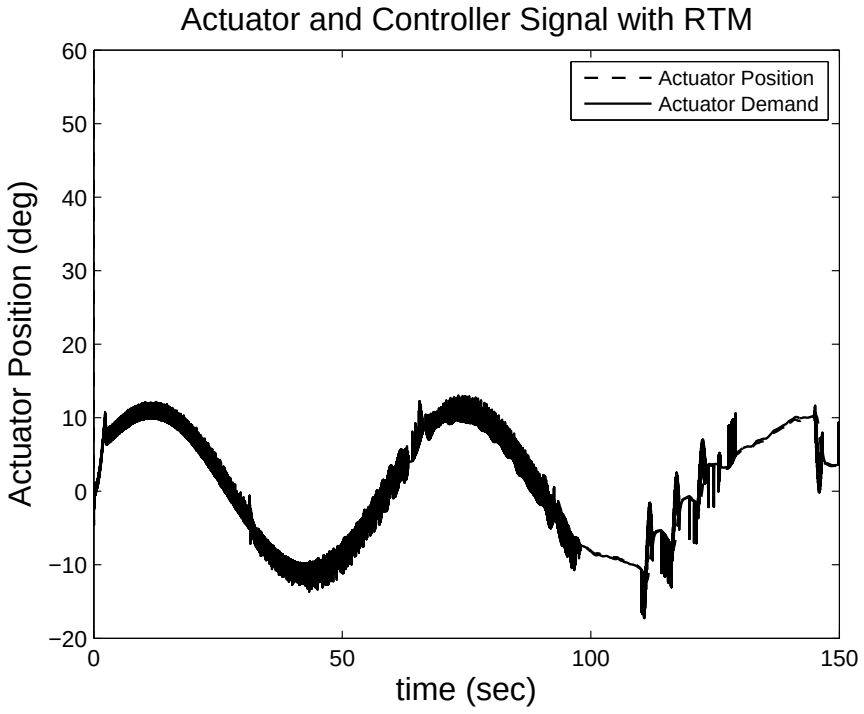

Figure 4.16. Actuator and controller response to modified trajectory r_{mod}.

without oscillations in spite of the fact that the modified trajectory is fairly close to the original reference.

CHAPTER 5

REFERENCE TRAJECTORY MODIFICATION USING AN EXTENDED KALMAN FILTER

5.1 Plant

In this Chapter the closed loop system components will be shown in state space form. The aircraft model can be shown in state space, where $x \in \mathbb{R}^4$, $u \in \mathbb{R}^1$, and $y \in \mathbb{R}^2$ are the state, control input, and output variables respectively. The system matrix A is obtained from [16]. The state equation is shown below

$$\begin{aligned} \dot{x} &= Ax + Bu \\ y &= Cx \end{aligned} \tag{5.1}$$

where, $A \in \mathbb{R}^{4\times4}$ and $C \in \mathbb{R}^{1\times4}$. The state variables of the fourth order system are the velocity, angle of attack, pitch angle and the pitch rate. The variables available for feedback are the angle of attack, α and the pitch rate, q.

5.2 Actuator and Controller

The CAS needed for precision tracking is implemented using a simple PID controller as shown in earlier chapters. The control gains used for the PID controller are determined from nominal system conditions.

The actuator model can be represented as follows:

$$\begin{aligned} \dot{x}_a &= f_a(x_a, u_c; p_a) \\ y_a &= h(x) \end{aligned} \tag{5.2}$$

where, $x_a \in \mathbb{R}^{n_a}$, $p_a \in \mathbb{R}^m$, $\delta \in \mathbb{R}^s$ represents the actuators states, actuators system parameters, and controller command respectively and $f \in \mathbb{R}^{n_a\times1}$ is a vector function.

The actuator is assumed to undergo failure such that the system parameters drift, in doing so the actuator model now becomes a time varying system shown as:

$$\dot{x}_{af} = f_f(x_{af}, p_{af}(t), u_c, t), \forall t \geq 0 \tag{5.3}$$

where the subscript f indicates post failure conditions. This failed actuator contains unknown time varying parameters $p_{af}(t)$ which must be estimated. No information is assumed to be known about the functions $p_{af}(t)$. The post-failure condition of the system must be detected and identified in real-time. In order to accomplish this, an EKF is proposed to identify the post failure conditions of the actuator system parameters.

5.3 Extended Kalman Filter

As shown in the previous chapter, the EKF can easily be developed by treating all unknown actuator parameters as additional states of the original model. In doing so, the augmented state vector is a combination of the original actuator states and unknown parameters. This changes the model from a time invariant to a time varying system. The new actuator variables are shown below:

$$x_A = \left\{ \begin{array}{c} x_a \\ \\ p_{af} \end{array} \right\} \tag{5.4}$$

and

$$\begin{aligned} \dot{x}_A &= f_A(x_A, u_c) \\ y_A &= h_A(x_A) \end{aligned} \tag{5.5}$$

where $x_A \in \mathbb{R}^{n_a+m}$ and $f_A \in \mathbb{R}^{n_a+m\times 1}$ is a vector function. A high frequency low amplitude signal is added in order to dither the system which improves the accuracy of the EKF. The output of the EKF generates the set of estimated parameters $\hat{p}_{at}(t)$.

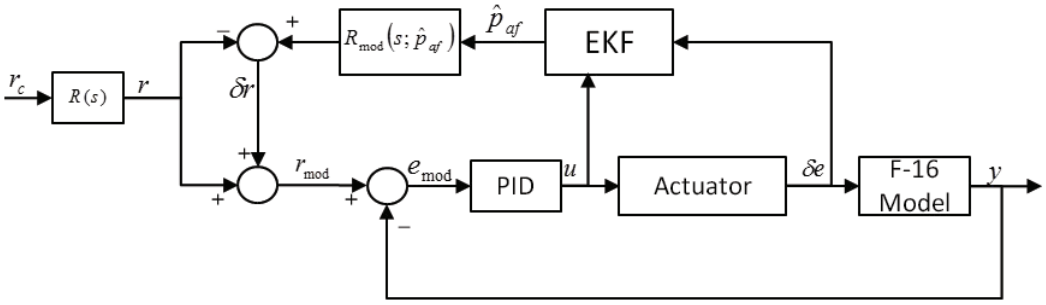

Figure 5.1. Modification Diagram.

5.4 Reference Modification

Now the actuator undergoes failure which causes the parameters to become time dependent which compromises the performance of the system. Therefore, the post failure error signal entering the closed loop system e_f is now providing inputs to the system that can cause instabilities or other undesired responses. In order to prevent this from occurring, the system must be adapted in such a way that after the failure takes place the reference command must account for the unexpected system changes. One approach is to add an additional signal to the summation junction where e is generated such that the new error signal e_{mod} is now within the allowed range of the system.

$$e_{mod} = r + \delta_r - y_r \tag{5.6}$$

and

$$r_{mod} = \delta_r + r \tag{5.7}$$

where δ_r is a function of the actuator parameters. $(\delta_r = \delta_r(x_A, t))$

5.5 Performance Evaluation of the Proposed RTM Scheme

The evaluation of the following scheme is demonstrated by a simple second order linear actuator model:

$$\begin{aligned} f_{1a} &= x_{2a} \\ f_{2a} &= -2\zeta\omega_n x_{2a} - {\omega_n}^2 x_{1a} \end{aligned} \tag{5.8}$$

Suppose the controller is given a pitch command r_c which is then shaped through a second order filter $R(s)$. The natural frequency of the filter under nominal conditions is designed to be 1/10 of that of the actuator. This guarantees that the generated reference pitch command $r(t)$ will be sufficiently slow for the actuator to track. The second order actuator is assumed to undergo failure such that the natural frequency and the damping ratio of the actuator is reduced. In doing so, the actuator now is a time varying system similar to that of Equation 5.5 which can be expressed as:

$$\begin{aligned} f_{1A} &= x_{2A} \\ f_{2A} &= -2x_{3A}x_{4A}x_{2A} - {x_{4A}}^2 x_{1A} \\ f_{3A} &= 0 \\ f_{4A} &= 0 \end{aligned} \tag{5.9}$$

r_{mod} will be set simply to maintain the original design parameter which set the frequency of r to be 1/10 of the actuator natural frequency. Therefore, $r_{mod}(s)$ will have the following form:

$$\ddot{r}_{mod} = -2\alpha_1\hat{x}_{3A}\hat{x}_{4A}\dot{r}_{mod} - (\alpha_1\hat{x}_{3A})^2 r_{mod} + (\alpha_1\hat{x}_{3A})^2 r_c \tag{5.10}$$

where $\alpha_1 = 0.1$. With the solution of Equation 5.10 one can now easily obtain δ_r from Equation 5.7.

5.6 Results

This heuristic approach to modifying the reference signal is shown to have certain benefits when dealing with varying parameters in the system.

Figures 5.2, and 5.3, shows the system experiencing failure during the simulation. Since the actuator bandwidth is dropping, it is expected that the system performance would deteriorate as the plant attempts to track the original reference trajectory. This simulation shows that as the actuator bandwidth drops below a certain point the system begins to oscillate and is no longer able to hold at the desired position. As additional inputs are generated by the actuator the systems oscillation amplitude increases. This increase drives the pitch response further away from the desired trajectory. Figure 5.3 shows the actuator response to the loss in bandwidth. The controller demand grows significantly in an attempt to reduce the system error $(r - y)$ to zero.

Figure 5.6 now includes the additional signal generated for trajectory modification. The new signal is now being tracked. This shows that the system's overall tracking performance does increase when the reference trajectory is modified by the proposed scheme.

The Figures 5.4 and 5.5 shows the performance of the EKF during RTM. Figure 5.5 shows the estimation of the damping ratio. This estimation loses accuracy during the simulation. This is due to the inadequate excitation of the input signal. A dither is added to the input in an attempt to improve the estimation. The natural frequency shown in Figure 5.4 is estimated accurately and effectively captures the degradation of the actuator. This estimation obtained from the EKF is used to developed the modified pitch rate reference.

Figures 5.6 shows the improvement of the plant output due to the modification of the reference trajectory. The dash-dot line shows the large oscillations in the

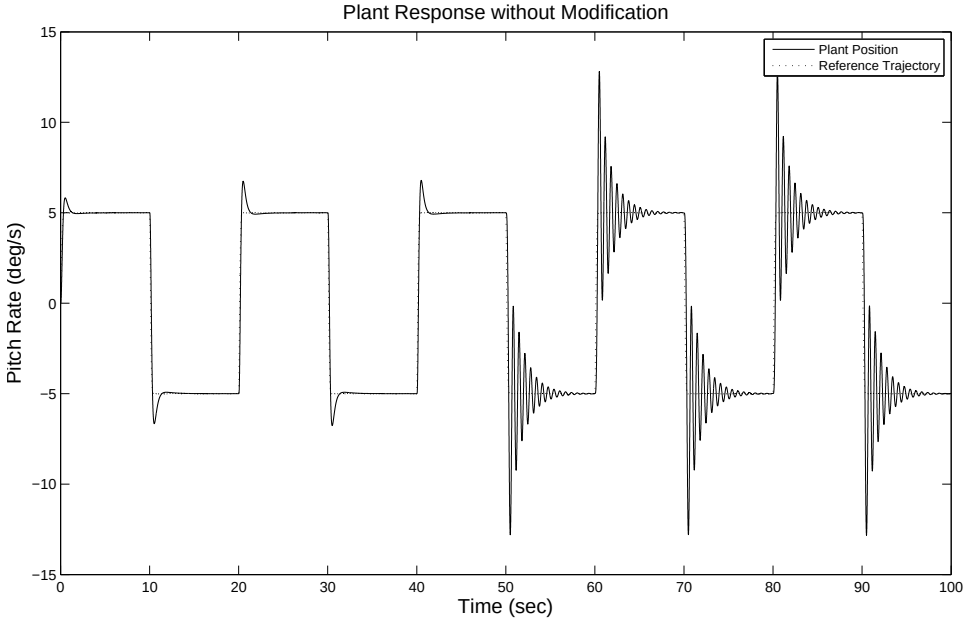

Figure 5.2. The effect of Parameter drift on plant output signal.

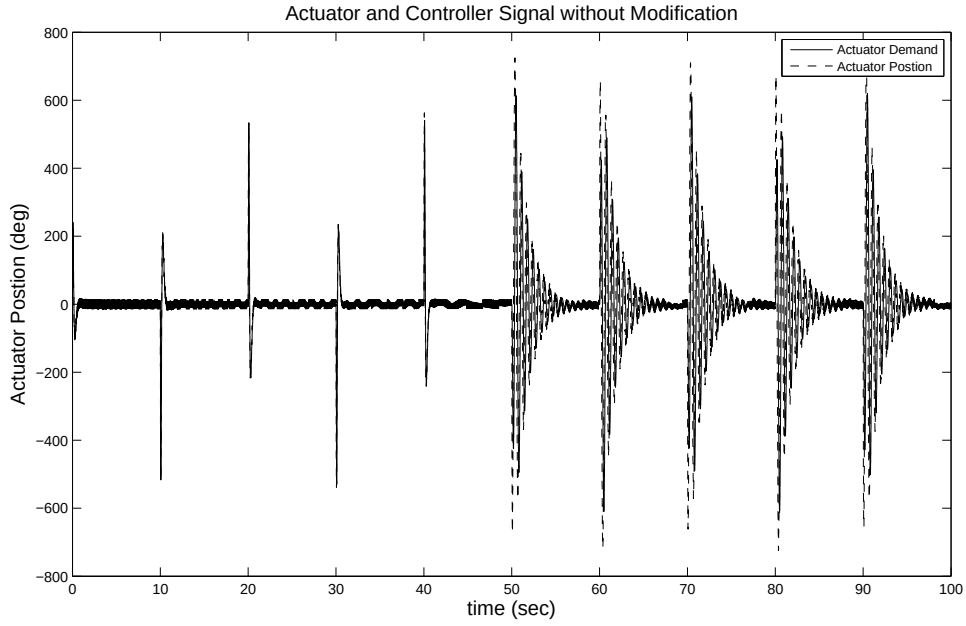

Figure 5.3. The effect of parameter drift on actuator response.

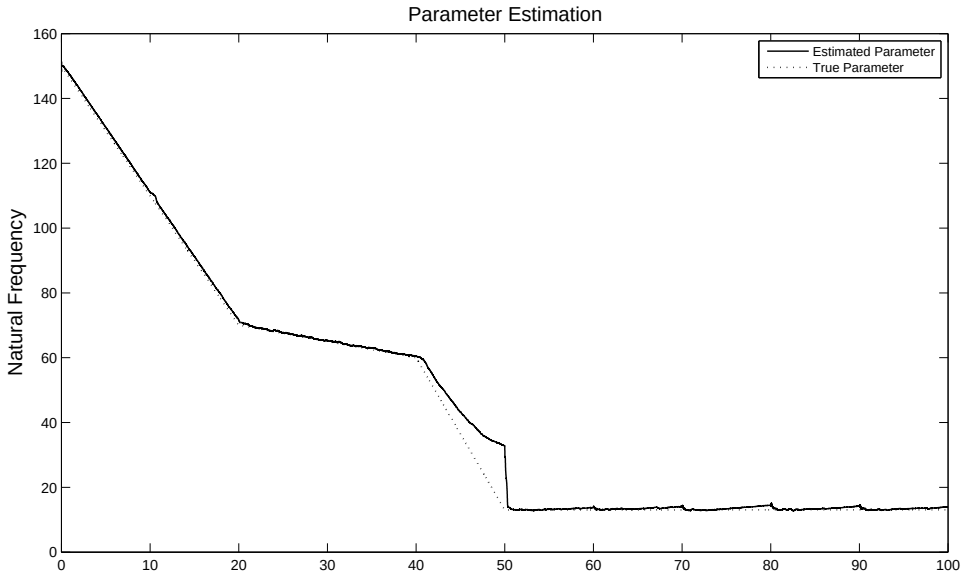

Figure 5.4. The EKF natural frequency estimation.

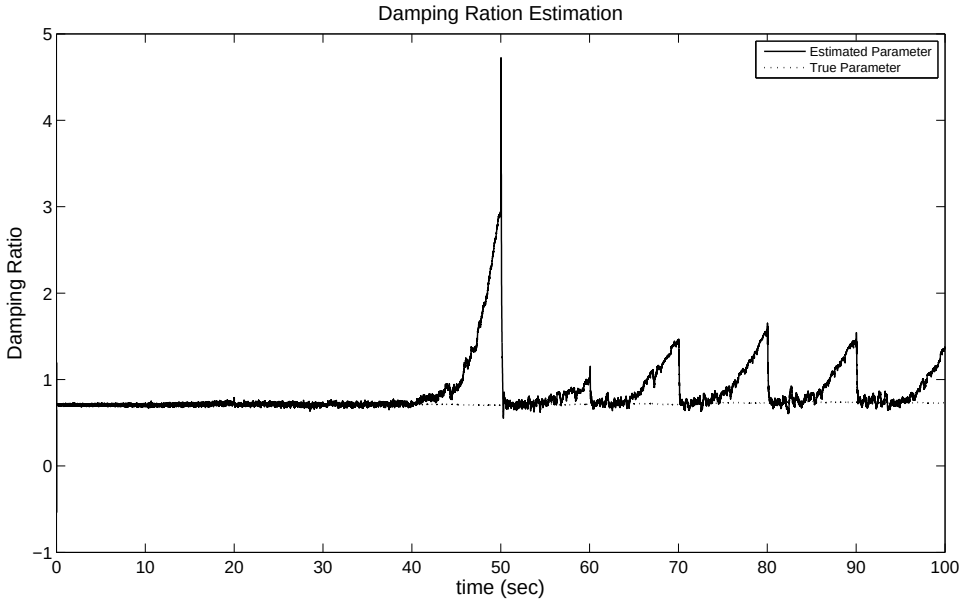

Figure 5.5. The EKF damping ratio estimation.

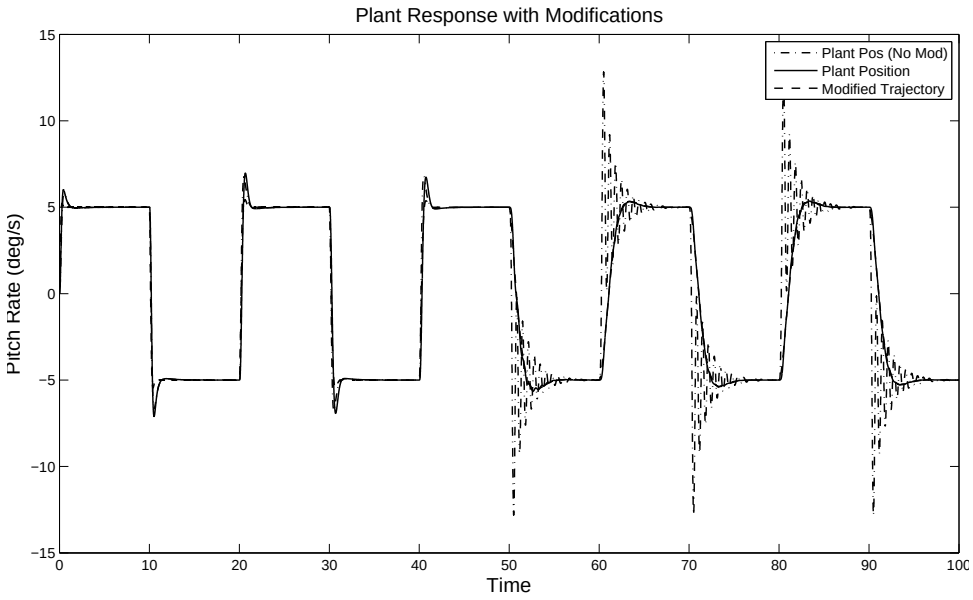

Figure 5.6. Plant Response to RTM.

original plant response. The solid line in the figure is the new plant output while tracking the modified reference created using the EKF to develop a modified reference. These results show that modifying the reference trajectory strictly reducing the natural frequency of $R(s)$ by a factor of what is estimated by the EKF serves to improve tracking performance.

CHAPTER 6

SUMMARY AND CONCLUSIONS

In this paper we showed an approach to accommodate real-time system failures. System performance is enhanced simply by reshaping or altering the input signal and it shows that complicated control law reconfiguration may be avoided.

The first method (RTM using Model Inversion) showed that for position saturation and the actuator can be account for without knowledge the actuator states. A simple model inversion of the actuator is all that is necessary to provide that closed loop system with a modified reference trajectory that will maintain stability and system performance. In order to implement a stable modification routine of this type, it is necessary to add filter prior to the model inversion.

The second method (RTM using Model Inversion and EKF) showed that this scheme can easily be extended to account for parameter drift in the actuator. In the case of unknown varying parameters an EKF was used for state estimation. This state estimation was used to recreated the actuator model which was then inverted in a similar manner as in the first method. Once the inversion is implemented the routine identical to that of the known actuator case and the modified trajectory can be easily generated.

The third method (RTM using EKF) showed an alternate approach to accommodating real time system failures using a simple EKF. System performance is enhanced simply by reshaping or altering the input signal and it shows that complicated control law reconfiguration may be avoided.

APPENDIX A

SYSTEM TRANSFER FUNCTIONS

In this appendix, we present the values used to generate the results shown.

A.1 Nominal Closed Loop System

$$A(s) = \frac{22500}{s^2 + 212.1s^2 + 22500} \tag{A.1}$$

$$P(s) = \frac{(-0.0021s - 0.1612); (-0.1755s - 0.1806)}{s^2 + 2.0963^s + 0.3536} \tag{A.2}$$

$$C(s) = 40 + \frac{1.5}{s} + 0.5s \tag{A.3}$$

The transfer function for the controller $C(s)$ is formed using the following PID gains. $K_p = 40, K_i = 1.5$ and $K_d = 0.5$.

The following equation is used to generate the nominal reference trajectory.

$$\texttt{Sinusoidal Reference } R(s) = \frac{2.625}{5s^2 + 2.65^2} \tag{A.4}$$

$$\texttt{Step Reference } R(s) = \frac{5}{s} \tag{A.5}$$

In order to create a constant excitation of the system modes for proper parameter identification a dither signal was superimposed on the nominal reference trajectory. The type of dither signal is shown in equation A.6

$$Dt(s) = \frac{0.06}{0.0001s^2 + 0.06^2} \tag{A.6}$$

A.2 System Failures

Table A.1 shows the values used to simulate actuator saturation failures.

Saturation Failures		
	Nominal Conditons	Post Failure Coniditon
Max Position	60 deg	6 deg
Posistion Error Time	NA	30sec

Figure A.1. Actuator failure and time.

In order to simulate the failure for loss of actuator bandwidth. The natural frequency and the damping ratio were reduced during the simulation. Figure A.2 shows the time history of the actuator parameters ζ and ω.

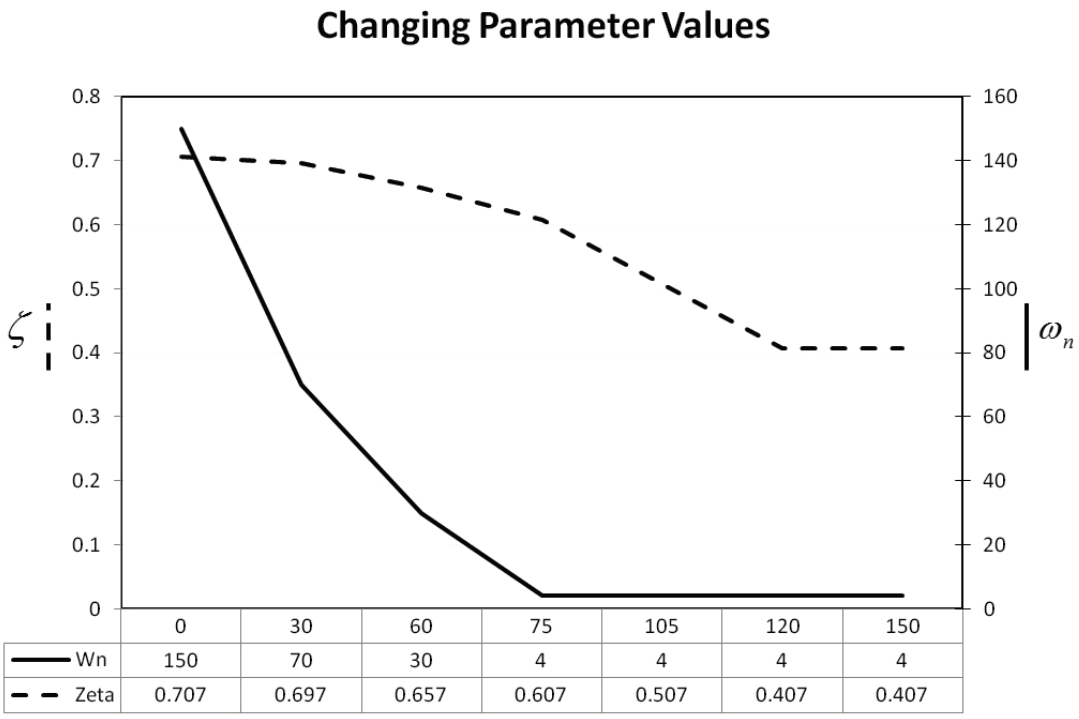

Figure A.2. Actuator failure and time.

APPENDIX B

EXTENDED KALMAN FILTER

In this appendix, we show how the extended Kalman filter is implemented in order to solve for the unknown actuator parameters. In order to initiate the filter certain constants and initial conditions must be set. This appendix shows the values of these terms.

B.1 EKF Formulation

Model

$$\begin{aligned} \dot{\mathbf{x}}_\mathbf{A} &= \mathbf{f}_\mathbf{A}(\mathbf{x}_\mathbf{A}, \mathbf{u}_\mathbf{c}) + G(t)\mathbf{w}(t), \mathbf{w}(t)\ N(\mathbf{0}, Q(t)) \\ \mathbf{y}_\mathbf{A} &= \mathbf{h}_\mathbf{A}(\mathbf{x}_\mathbf{A}) + \mathbf{v}(t), \mathbf{v}(t)\ N(\mathbf{0}, Q(t)) \end{aligned} \tag{B.1}$$

Equation 5.5 gives the expression for the system model shown in B.1. The model that was simulated in simulink is shown in equation B.2

$$\begin{aligned} \dot{x}_{A1} &= x_{A2} \\ \dot{x}_{A2} &= 2x_{A1}x_{A2}x_{A3}x_{A4} \\ \dot{x}_{A3} &= 0 \\ \dot{x}_{A4} &= 0 \end{aligned} \tag{B.2}$$

where,

$$G(t) = 0.5 \begin{bmatrix} 1 & 0 & 0 & 0 \\ 0 & 1 & 0 & 0 \\ 0 & 0 & 1 & 0 \\ 0 & 0 & 0 & 1 \end{bmatrix} \tag{B.3}$$

$$\mathbf{w}(t) = 0.1 \begin{bmatrix} 0.05 \\ 0.05 \\ 0.05 \\ 0.05 \end{bmatrix} \tag{B.4}$$

$$Q(t) = 2 \begin{bmatrix} 1 & 0 & 0 & 0 \\ 0 & 1 & 0 & 0 \\ 0 & 0 & 1 & 0 \\ 0 & 0 & 0 & 1 \end{bmatrix} \tag{B.5}$$

$$\mathbf{v}(t) = 0.01 \begin{bmatrix} 0.01 \\ 0.01 \\ 0.01 \\ 0.01 \end{bmatrix} \tag{B.6}$$

and,

$$R(t) = 0.0002 \begin{bmatrix} 1 & 0 & 0 & 0 \\ 0 & 1 & 0 & 0 \\ 0 & 0 & 1 & 0 \\ 0 & 0 & 0 & 1 \end{bmatrix} \tag{B.7}$$

Initialization

$$\begin{aligned} \hat{\mathbf{x}}_{\mathbf{A}}(t_0) &= \hat{\mathbf{x}}_{\mathbf{A0}} \\ P_0 &= E\left\{\tilde{\mathbf{x}}_{\mathbf{A}}(t_0)\tilde{\mathbf{x}}_{\mathbf{A}}^{\mathbf{T}}(t_0)\right\} \end{aligned} \tag{B.8}$$

The initialization equation shows the expression for the initial estimates for the EKF. The initial estimates that were chosen are shown below.

$$\hat{\mathbf{x}}_{\mathbf{A}}(t_0) = \begin{bmatrix} 0.1 \\ 0.1 \\ 149 \\ 0.65 \end{bmatrix} \tag{B.9}$$

and,

$$P_0 = 1000 \begin{bmatrix} 1 & 0 & 0 & 0 \\ 0 & 1 & 0 & 0 \\ 0 & 0 & 1 & 0 \\ 0 & 0 & 0 & 1 \end{bmatrix} \tag{B.10}$$

APPENDIX C

SIMULINK MODELS

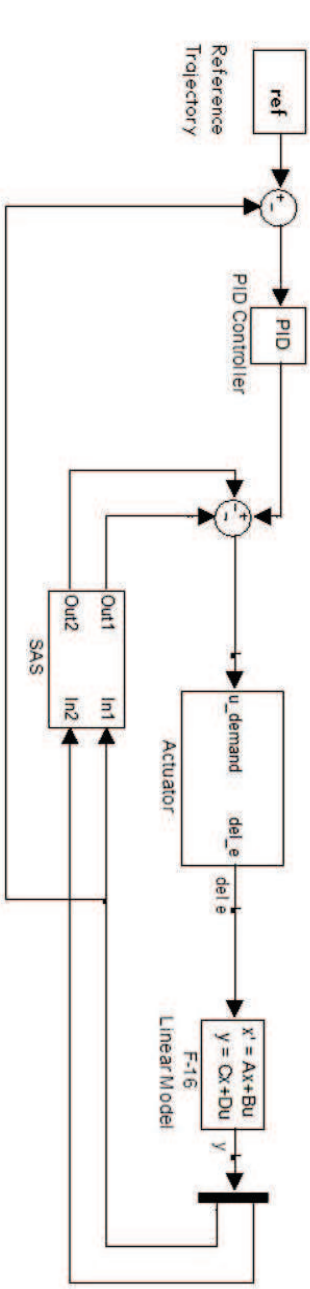

Figure C.1. The diagram of the nominal system that was used for the simulation.

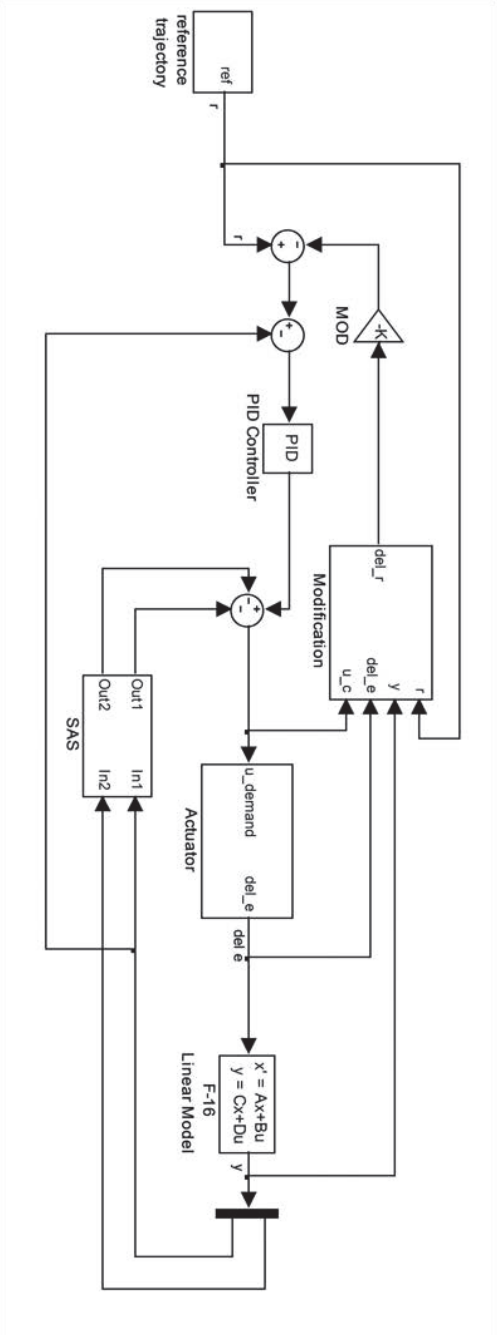

Figure C.2. The diagram of the Simulink model that was used for the model inversion method to generate a modified reference trajectory.

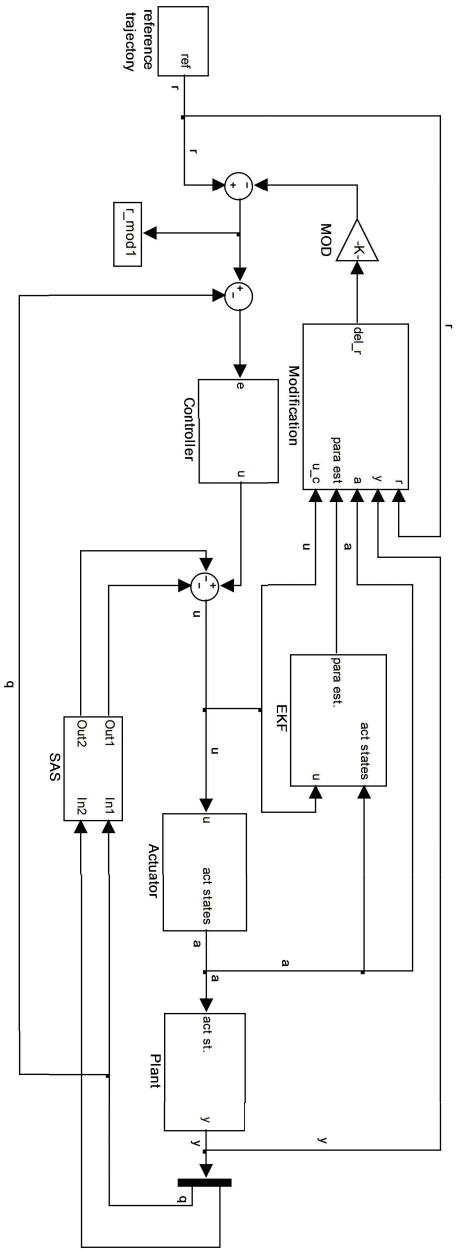

Figure C.3. The diagram of the Simulink model that was used for the model inversion and EKF method to generate a modified reference trajectory.

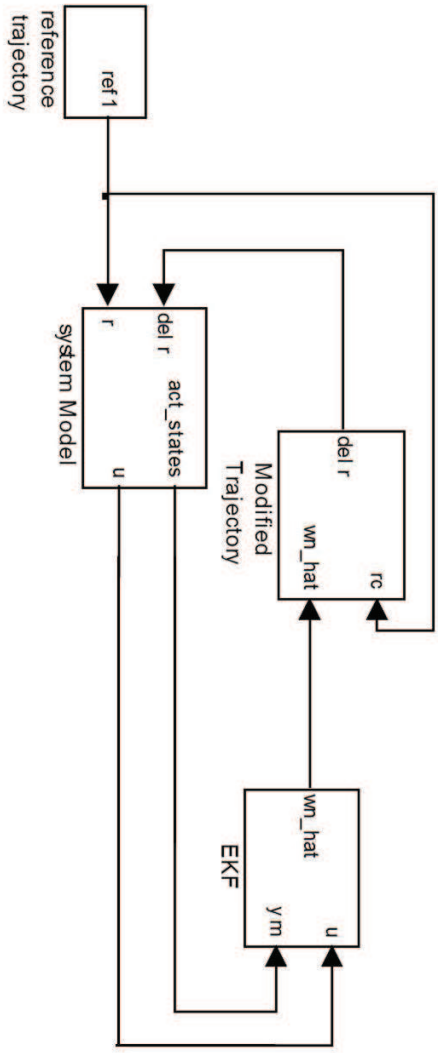

Figure C.4. The diagram of the Simulink model that was used for the model EKF only method to generate a modified reference trajectory.

REFERENCES

[1] J. D. Boskovic, S. E. Bergstrom, and R. K. Mehrak, "Robust integrated flight control design under failures, damage, and state-dependent disturbances."

[2] S. Jung and Hsia, "On reference trajectory modification approach for cartesian space neural networks control of robot manipulators," *Robotics and Automation, 1995. Proc. of IEEE International Conference*, vol. 1, pp. 575–580, May 21–27, 1995.

[3] E. N. Johnson and A. J. Calise, "Pseudo-control hedging: A new method for adaptive control," in *Proc. Advances in Navigation Guidance and Control Technology Workshop*, REdstone Arsenal, Alabama, Nov.1–2, 2000.

[4] A. Glattfelder and W. Schaufelberger, *Control Systems with Input and Output Constraints*. London: Springer-Verlag, 2003.

[5] J. D. Boskovic, J. Redding, and R. K. Mehra, "Integrated health monitoring and adaptive reconfigurable control," in *Proc. AIAA Guidance, Navigation, and Control Conference and Exhibit*, Hilton Head, South Carolina, Aug. 20–23, 2007.

[6] D.-H. Shin and Y. Kim, "Reconfigurable flight control system design using adaptive neural networks," *IEEE Transactions on Control Systems Technology*, vol. 12, no. 1, Jan 2004.

[7] C. Cao and N. Hovakimyan, "Design and analysis of a novel l1 adaptive controller, part 1: Control signal and asymptotic stability," in *Proc. of the 2006 American Control Conference*, Minneapolis, Minnesota, June 14–16, 2006.

[8] X. Wang and V. L. Syrmos, "Design of adaptive reconfigurable control systems using extended kalman filter-bases system identification and eigenstructure as-

signments," *Smart Structures and Materials: Modeling, Signal Processing, and Control*, vol. 5383, Dec 2004.

[9] P. Singla and K. Subbarao, "Stable adaptive reference trajectory modification for saturated spacecraft control applications," in *Proc. IEEE 2008 American Control Conference*, paper Paper No. 99-4241.

[10] R. Hess, W.Siwakosit, and J. Chun, "Accommodating actuator failures in flight control systems," in *37th AIAA Aerospace Sciences Meeting and Exhibit*, Reno, NV, Jan. 11–14, 1999, paper AIAA Paper No. 99-0634.

[11] M. D. Tandale and J. Valaek, "Adaptive dynamic inversion control with actuator saturation constraints applied to tracking spacecraft maneuvers," *The Journal of the Astronautical Sciences*, vol. 52, no. 4, Dec 2004.

[12] I. Ogunleye and K. Subbarao, "Stable reference trajecjory modification for handling actuator saturation in control systems,," in *Proc. Info Tech*, St. Louis, Missouri, Mar. 15–18, 2011, paper AIAA 2005-6436.

[13] M. W. Oppenheimer and D. B. Doman, "On-line adaptive estimation and trajectory reshaping," in *Proc. AIAA Guidance, Navigation, and Control Conference and Exhibit*, San Francisco, California, Aug. 15–18, 2005, paper AIAA 2005-6436.

[14] W. Siwakosit and R. Hess, "A reconfiguration scheme for accommodating actuator failures in multi-input, multi-output flight control systems," in *AIAA Guidance, Navigation, and Control Conference and Exhibit*, Denver, CO, Aug. 11–14, 2000.

[15] E. N. Johnson and A. J. Calise, "Inverse dynamics approach for real-time determination of feasible aircraft reference trajectories," in *AIAA Guidance, Navigation, and Control Conf. and Exhibit*, paper Paper No. 99-4241.

[16] B. L. Steven and F. L. Lewis, *Aircraft Control and Simulation*, 2nd ed. New Jersey: John Wiley and Sons, Inc., 2003.

[17] V. Kapila and K. M. Grigoriadis, *Actuator Saturation Control*. Marcel Dekker, Inc, 2003.

[18] J. L. Crassidis and J. L. Junkins, *Optimal Estimatioin of Dynamic Systems*. Chapman and Hall CRC, 2004.

[19] E. N. Johnson and A. J. Calise, "Pseudo-control hedging: A new method for adaptive control," in *Advances in Navigation Guidance and Control Technology Workshop*, Redstone Arsenal, Alabama, Nov. 1–2, 2006.

[20] J. D. Schierman, D. G. Ward, J. R. Hull, and N. Gandhi, "Intelligent guidance and trajectory command systems for autonomous space vehicles," in *Proc. AIAA 1st Intelligent Systems Technical Conference*, Chicago, Illinois, 20–22, 2004, paper AIAA 2004-6253.

[21] M. B. Milam, K. Mushambi, and R. M. Murray, "A new computational approach to real-time trajectory generation for constrained mechanical systems," in *Proc. AIAA 1st Intelligent Systems Technical Conference*, Chicago, Illinois, 20–22, 2004, paper AIAA 2004-6253.

[22] J. D. Schierman, J. R. hull, N. Gandhi, and D. G. Ward, "Flight test results of an adaptive guidance system for reusable launch vehicles," in *Proc. AIAA Guidance, Navigation, and Control Conference and Exhibit*, Providence, Rhode Island, Aug. 16–19, 2004, paper AIAA 2004-4771.

[23] J. D. Boskovic, J. Redding, and R. K. Mehra, "Fast on-line actuator reconfiguration enabling (flare) system," in *Proc. AIAA Guidance, Navigation, and Control Conference and Exhibit*, Hilton Head, South Carolina, Aug. 15–18, 2005.

[24] S. Jung and T. C. Hsia, "On reference trajectory modification approach for cartesian space neural networks control of robot manipulators," *Robotics and Automation, 1995. Proceedings of IEEE International Conference*, vol. 1, no. 1, Jan 1995.

[25] L. A. Calise and M. Sharma, "Direct adaptive reconfigurable control of a tailless fight aircraft," in *AIAA Guidance, Navigation, and Control Conference*, USA, Aug.1–2, 1998.

[26] V. Bararic, Z. Vukic, and R. Antonic, "Scope and application of reconfigurable control," in *Proc. Mediterranean Conference on Control and Automation*, Rhodes, Greece, 18–20, 2003.

[27] L. Wills, S. Kannan, S. Sander, M. Guler, B. Heck, J. Prasad, D. Schrage, and G. Vachtsevanos, "An open platform for reconfigurable control," *IEEE Control Syst. Mag*, vol. 21, pp. 49–64, June 2001.

[28] L. Drolet, F. Michaud, and J. Cote, "Adaptable sensor fusion using multiple kalman filters," in *IEEE/RSJ Int. Conf. on Intelligent Robots and Systems (IROS)*, 2000.

[29] T.-A. Pham, "Validation and verification of aircraft control software for control improvement," Master's thesis, Department of Computer Science San Jose State University, 2007.

[30] A. Mili, B. Cukic, Y. Liu, and R. B. Ayed, "Towards the verification and validation of online learning systems: General framework and applications," in *in Proc. of the 37th Annual Hawaii International Conference on System Sciences (HICSS'04)*, vol. 9, 2004.

[31] D. Bedford, G. Morgan, and J. Austin, "Requirements for a standard certifying the use of artificial neural networks in safety critical applications," in *International Conference on Artificial Neural Networks*, Bochum, Germany, 1996.

[32] C. Gao and R. Hess, "Inverse simulation of large-amplitude aircraft maneuvers," *Journal of Guidance, Control, and Dynamics*, vol. 16, no. 4, pp. 733–737, 1993.

[33] J. Junkins and Y. Kim, "Stability and control of robotic space manipulators," in *Teleoperation and Robotics in Space*, S. B. Skaar and C. F. Ruoff, Eds., vol. 161,

no. 315-350, AIAA. Washington DC: Progress in Astronautics and Aeronautics, 1995.

[34] R. Rysdyk, "Adaptive nonlinear flight control," Ph.D. dissertation, Georgia Institute of Technology, 1998.

[35] M. McFarland and A. Calise, "Adaptive nonlinear control of agile antiair missiles using neural networks," *IEEE Transactions on Control Systems Technology*, vol. 8, pp. 749–756, Sep 2000.

[36] Y. Peng, D. Vrancic, and R. Hanus, "Anti-windup, bumpless, and conditioned transfer techniques for pid controllers," *IEEE Control Systems*, 1996.

BIOGRAPHICAL STATEMENT

Ifeolu O Ogunleye was born in Lagos, Nigeria, in 1982. He received his B.S. degree from The University of Texas Arlington in 2005 and M.S. degree from The University of Texas at Arlington in 2011 all in Aerospace Engineering. From 2003 to 2011, he was with the Department of Defense employed with the Defense Contract Management Agency at the Lockheed Martin Aeronautics Company in Fort Worth Texas working as an Aerospace Engineer. His time there was spent working on several different DoD contracts. In 2011, he joined the Federal Aviation Administration as an Aerospace Engineer working on the type certification and developing regulations of Advanced Electrical Flight Systems such as autopilots, advanced flight control systems, and GPS Navigation Systems. His current research interest is in the area of real flight control configuration.